

The Positron Puzzle

Thomas Siebert^{1*}

^{1*}Julius-Maximilians-Universität Würzburg, Fakultät für Physik und Astronomie, Institut für Theoretische Physik und Astrophysik, Lehrstuhl für Astronomie, Emil-Fischer-Str. 31, D-97074 Würzburg, Germany.

Corresponding author(s). E-mail(s): thomas.siebert@uni-wuerzburg.de;

Abstract

The Positron Puzzle is a half-century old conundrum about the origin of the Galactic γ -ray emission line at photon energies of 511 keV, and the shape of its morphology, showing a bulge-to-disk luminosity ratio of ~ 1 – unlike any astrophysical source distribution. Positrons (e^+ s) that have been cooled to the eV scale capture electrons (e^- s) and form the intermediate bound state of Positronium (Ps) which decays on a nano-second timescale into two or three photons. Assuming the emission to originate from the Galactic bulge, centre, and disk, a *visible* annihilation rate in the Milky Way of $\sim 5 \times 10^{43} e^+ s^{-1}$ has to be explained, either by a quasi-steady state of production and annihilation, or by possibly multiple burst-like events that flood the Galaxy with e^+ s, then fading away on a Myr timescale.

In this paper, I will review what the real Positron Puzzle is, where data and simulations have been used inadequately which resulted in false claims and an apparent quandary, what we really know and absolutely not know about the topic, and how this epistemic problem might be advancing.

Keywords: Positrons, Cosmic rays, Gamma rays, Interstellar medium, Dark matter

1 Introduction

1.1 What do we see?

The Galactic 511 keV signal has been measured with multiple instruments for the last 50 years. Acknowledging the pioneering balloon experiments in the 1960s and '70s (Haymes et al, 1969), as well as the first identification of its ‘diffuse’ nature with satellite experiments in the '90s (CGRO/OSSE, Purcell et al, 1997) (see also (Albernhe et al, 1981; Lingenfelter and Ramaty, 1989)), the most extensive information in this topic has been gathered from INTEGRAL/SPI measurements (Winkler et al, 2003; Vedrenne et al, 2003). With increasing exposure time since

2002, SPI measurements allowed us to refine earlier conjectures about its possible dark matter (DM, Boehm et al, 2004) origin, conditions as to how e^+ s annihilate (e.g., Jean et al, 2006; Churazov et al, 2005; Siebert et al, 2019a), and tried to infer whether, and if how far, e^+ s propagate (e.g., Jean et al, 2009; Martin et al, 2012; Alexis et al, 2014; Siebert et al, 2022c). The image that we can obtain with SPI at 511 keV photon energies is unique compared to other wavelengths and emission processes (Fig.1). The latest measurement of 511 keV fluxes in the Galaxy are from Skinner et al (2014) and Siebert et al (2016b), finding $F_B = (8.9\text{--}10.1) \times 10^{-4} \text{ ph cm}^{-2} \text{ s}^{-1}$, $F_D = (13.1\text{--}20.1) \times 10^{-4} \text{ ph cm}^{-2} \text{ s}^{-1}$, and $F_{GCS} = (0.6\text{--}1.2) \times$

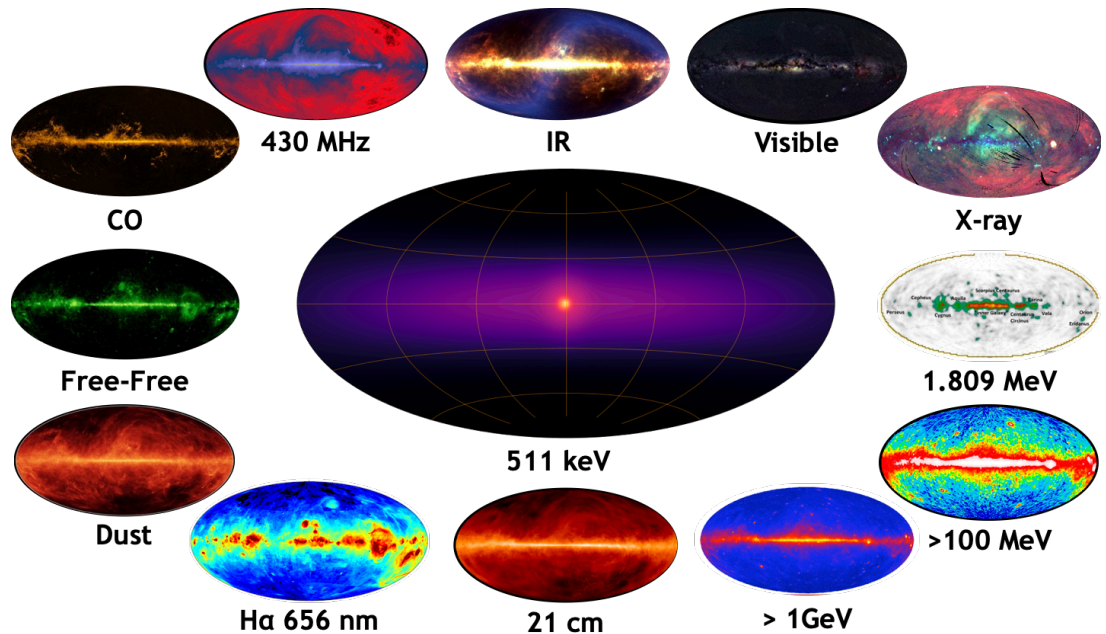


Fig. 1 Full-sky maps at different wavelengths and emission processes compared to a maximum likelihood solution from INTEGRAL/SPI data at 511 keV (Siegert et al, 2016b).

10^{-4} ph cm $^{-2}$ s $^{-1}$ for the Galactic bulge, disk, and centre, respectively. The flux ratio between the bulge and disk emission is $F_B/F_D = 0.6 \pm 0.1$ (Skinner et al, 2014; Siegert et al, 2016b), which results in a luminosity ratio of $L_B/L_D = 1.0 \pm 0.1$ when assuming an effective distance to the bulge of 8.2 kpc and to the disk of 6.5 kpc (Siegert et al, 2016b). Historically, the bulge-to-disk ratio was even larger because the disk was not detected in earlier measurements with SPI with less exposure time (e.g., Knoedlseder et al, 2005; Bouchet et al, 2010). It is not excluded that the disk may actually not be *the* Galactic disk, but rather halo emission or even foreground. In the latter two cases, inferences with SPI would suffer from its coded aperture mask design, being almost incapable of measuring isotropic emission or shallow gradients (Caroli et al, 1987; Siegert et al, 2022d). In addition, Siegert et al (2019b) showed that there is hardly a trend of Doppler-shifts in the 511 keV line along Galactic longitudes, which would verify a rotation curve and the extended emission beyond the bulge as *the* Galactic disk. Certainly, e^+ s at the MeV scale are produced inside the Galactic disk (Sec. 2.2), but how far they propagate, where they finally annihilate, and at what rate is a matter of debate (see also the works by

Prantzos (2006) and Higdon et al (2009) for more details about a possible scenario to channel e^+ s from the disk to the bulge).

The central map in Fig. 1 shows a maximum likelihood fit to the raw SPI count data, requiring four components: a disk, and three components to describe the bulge, including a point-like source coincident with the Galactic centre. Note that the angular resolution of SPI is 2.7° , so that this point source encompasses about 400 pc in diameter – reminiscent of the entire Central Molecular Zone. The bulge component also shows an asymmetry, peaking around $l = -1^\circ$, which is consistently found in different analyses with different states of accumulated exposure (Weidenspointner et al, 2000; Bouchet et al, 2010; Skinner et al, 2014; Siegert et al, 2016b, 2022c). Structured, i.e. more granular images from reconstruction algorithms show a similar trend of where the flux is enhanced, and could reveal details if were it not for the strong instrumental background in MeV telescopes. While the basic structure is also found with Richardson-Lucy (Knoedlseder et al, 2005), Maximum Likelihood (Bouchet et al, 2010), or Maximum Entropy (Siegert, 2017) deconvolutions, image artefacts naturally emerge from the finite number of photons detected and to be distributed

over a large number of pixels. High-resolution spectroscopy of the 511 keV line for the bulge and disk components suggests that the annihilation of e^+ s occurs dominantly in the interstellar medium (ISM), which would partly explain the ‘diffuse’ nature of the image:

1.2 Positron annihilation spectroscopy

Previous works (e.g., Churazov et al, 2005, 2011; Jean et al, 2006; Guessoum et al, 2005, 2010; Siegert et al, 2016b) consistently find that, assuming e^+ s annihilate in the ISM, the temperature and ionisation state of the gas in which they are annihilating is 7000–40000 K and 2–25 %, respectively. The dominant annihilation process is then charge exchange with neutral and moderately warm gas. Charge exchange, for example with hydrogen, is only possible if the e^+ s have a kinetic energy of at least 6.8 eV (binding energy of H minus the binding energy of Ps), which would correspond to an ISM temperature of 80000 K. If e^+ s reach the temperature of the ISM, they ‘thermalise’, i.e. they are relaxing their kinetic energies to that of a Maxwellian distribution, so that the energy thresholds can be overcome only in the tail of the distribution. One model that fits the narrow and broad 511 keV line in the Milky Way is described as 49 % annihilation in the warm neutral phase and 51 % in the warm ionised phase (Jean et al, 2006): In the ionised phase, e^+ s annihilate after thermalisation by the formation of Ps via radiative recombination with free e^- s (no energy threshold), and to a lesser extent direct annihilation with e^- s, forming a ~ 1 keV broad line (FWHM), without any Ps formation in flight. In the warm phase, most e^+ s form Ps in flight, resulting in a $\gtrsim 6$ keV broad line, and a small percentage thermalises, again forming Ps, now with a narrow ~ 1 keV line. The total Ps fraction,

$$f_{\text{Ps}} = \frac{8r_{32}}{9 + 6r_{32}}, \quad (1)$$

with $r_{32} = F_{\text{oPs}}/F_{511}$ being the flux ratio between the ortho-Ps continuum and the 511 keV line, describes the fraction of e^+ s that undergo the formation of Ps (e.g., Leventhal et al, 1978). In the warm ionised medium f_{Ps} is $\sim 88\%$ and in the warm neutral medium $\sim 100\%$, resulting in a

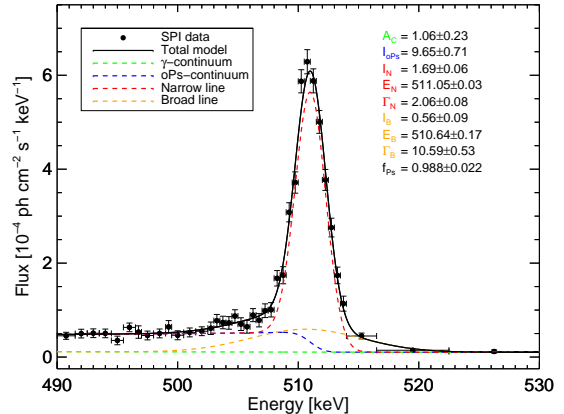


Fig. 2 INTEGRAL/SPI spectrum of the entire Galaxy, decomposed into a narrow and a broad line, in addition to the ortho-Ps continuum and the Galactic diffuse continuum (Siegert et al, 2019a).

total Ps fraction across the Galaxy of 92–97 %. In fact, some of the broadening of the Galactic 511 keV line may also be due to velocity broadening from Galactic rotation (Siegert et al, 2019a). Furthermore, the line is not the only witness of annihilating e^+ s: the ortho-Ps component (Ore and Powell, 1949) is also clearly visible in the combined spectra across the Galaxy, rising almost linearly with a sharp cut off at 511 keV, and containing a ≈ 4 times larger annihilation flux, depending on f_{Ps} (Fig. 2).

All these assumptions make perfect sense, if the premise of ‘annihilation in the ISM’ is correct. However, the density of target particles also has a considerable impact on the line shape and Ps fraction, once the densities of the gas is much higher than that of the ISM: Murphy et al (2005) calculate the Ps fraction as a function of temperature and gas density in the context of solar flares, finding that ~ 1 keV broad 511 keV lines can be explained in gas with densities $\gtrsim 10^9 \text{ cm}^{-3}$ and temperatures $\lesssim 2 \times 10^4$ K. Also the broad-to narrow-line ratio is found to be below 2 for temperatures above ~ 8000 K. Finally, the Ps fraction, albeit on the lower side, can also be met in conditions typical of solar flares.

1.3 A puzzling picture

The ‘Positron Puzzle’ may be summarised in three basic questions:

1. What do we see?

2. Where do the positrons come from?
3. Why does it look like that?

The answer to the first question, albeit somewhat ambiguous considering the limitations of current instrumentation in the MeV γ -ray band, is outlined in Secs. 1.1 and 1.2. Measurements in the MeV regime suffer from a scarcity of photons from astrophysical sources, carrying a million times more energy in one quantum than optical photons, for example, large instrumental background (Diehl et al, 2018; Siegert et al, 2019b), and apertures which align more with particle detectors in space rather than telescopes (Siegert et al, 2022d). Images are therefore often either ‘reconstructed’, i.e. it is attempted to unfold the non-invertible imaging response matrices of MeV instruments, or models are directly fitted to the raw data. In performing these imaging techniques, however, comparisons to other wavelengths, that could be more directly measured, can result in false conclusions. But in addition to the imaging capabilities, also the spectroscopic information of the 511 keV line will help to decipher ‘how’ the e^+ s are annihilating. In the paragraphs in Sec. 1.4, I outline possible tracers of e^+ -annihilation, based on first, the visual comparison of all-sky surveys from Fig. 1, and second, a thorough likelihood comparison.

The second question is the historically initial question after Leventhal et al (1978) unambiguously identified the γ -ray line from the Galactic centre as due to e^+ -annihilation. “*Undoubtedly, the positrons giving rise to the observed feature come from a variety of processes*”, said Leventhal et al (1978) about this first and strongest γ -ray line detected. Indeed, where the e^+ s come from, i.e. in which astrophysical sources they originate, is related to how e^+ s can be produced in terms of particle physics processes. I will summarise possible e^+ sources and production mechanisms in Sec. 2, together with measurements of how much which source population might contribute to the Galactic e^+ budget.

But the budget alone is not enough to gain complete insight into the ‘Positron Puzzle’ because the sources of e^+ s may in fact not be the sinks of e^+ annihilation. This is related to the third question of why the emission looks so different than the putative sources, and also different to the supposedly preferred annihilation regions

of dense gas in the Milky Way. Positrons are typically produced at mildly- or highly-relativistic energies (see Sec. 2). This means, unless they experience favouring annihilation conditions, such as high gas or e^- densities and low temperatures, they *are* cosmic rays, and propagate through the ISM. In Sec. 3, I will summarise the current knowledge of propagation of e^+ s in the ISM, which links to the distortion of the potential source distributions towards the measured 511 keV image. The injection of e^- s and e^+ s into the ISM will transport the particles on timescales of 0.1–10 Myr to distances (path lengths) of 0.1–10 kpc away from their initial sources (e.g., Jean et al, 2009; Panther, 2018). Consequently, to first order, the 511 keV image could be a smeared-out version of the initial source distribution due to the propagation effects, which may be similar to the gas distribution of the Galaxy.

The Milky Way can either be described in terms of its stellar population (putative e^+ sources) or in terms of its gas content (possible e^+ annihilation regions). The stellar population can be subdivided in the Galactic bulge and the Galactic disk (Freudenreich, 1998). The bulge shows a scale size of ~ 1.6 kpc, an old stellar population (~ 10 Gyr), and a stellar mass of $\sim 1.5 \times 10^{10} M_\odot$. The disk can be divided further into a thin (young(er) stars, on average ~ 5 Gyr) with scale height and radius of ~ 300 pc and 2.6 kpc, respectively, and a thick disk (old stars, ~ 10 Gyr) with scale height and radius of 900 pc and 3.6 kpc, respectively. The stellar masses of the thin and thick disk are ~ 2.5 and $\sim 0.5 \times 10^{10} M_\odot$, respectively. The gas in the Galaxy can be roughly subdivided into a molecular, an atomic, and an ionised component, with scale heights of ~ 50 pc (Dame et al, 2001), ~ 100 pc (Dickey and Lockman, 1990), and ~ 1800 pc (Gaensler et al, 2008), respectively. The total gas mass of the disk (2–20 kpc) is on the order of $10^{10} M_\odot$, similar to that of the bulge gas mass (Ferrière, 2001; Ferrière et al, 2007). In addition to the bulge and disk gas reservoirs, there is also the Central Molecular Zone (CMZ, Morris and Serabyn, 1996) encompassing the Galactic centre. It is ~ 400 pc in size with a strong concentration of molecular gas.

1.4 Positron annihilation tracers

With the information above, we can investigate Fig. 1 for tracers of e^+ annihilation:

Ionisation:

Ionisation and recombination of hydrogen (Seaton, 1959), as would happen as a consequence of the charge exchange process and radiative recombination with e^- s, may be traced in the ISM by $H\alpha$ in the Milky Way at photon wavelengths of 656 nm (Finkbeiner, 2003). The $H\alpha$ emission appears clumpy with several hotspots along the Galactic plane as well as nearby star forming regions, such as Orion, Scorpius Centaurus, Cygnus, Carina, or Vela. There is no definite bulge emission that would outshine the disk, and the bulge-to-disk ratio is tiny.

Warm ISM:

The distribution of neutral and partly warm gas in the Milky Way is visible in the 21 cm line of atomic hydrogen (HI; e.g., Kerp et al, 2011). The emission is concentrated in a thin disk along the Galactic plane with visible cavities, so-called superbubbles (Weaver et al, 1977; Castor et al, 1975), that have been formed by massive star winds and supernovae (SNe) over Myr timescales. The cavities may extend to several kpc above the Galactic plane so that the total HI emission may be described by a thin and a thick disk. The map shows where the gas might be found for the e^+ s to annihilate in, but there is no bright bulge at 21 cm wavelengths.

Cold ISM:

Based on logic arguments and reasonable estimates for the lifetime of e^+ s in the ISM (Panther et al, 2018b), the higher the density of the ISM, the more e^+ s should be seen to annihilate. The CO map ($J = 1 \rightarrow 0$ transition, Dame et al, 2001) at 115 GHz shows the dense and cold gas – regions where e^+ s should naturally tend to reach for annihilation if not quenched by too low temperatures to undergo charge exchange. The thin disk of CO is nothing like the 511 keV map, and also no bulge is present. However, the CMZ would be coincident with the point-like source at 511 keV.

Dust grains:

It appears that annihilation on dust grains is not excluded by the spectral data although the emission morphology, again, would be disfavoured by direct comparison of the dust map (e.g., Bennett et al, 2013; Planck Collaboration et al, 2016) in Fig. 1 to the 511 keV map. Also PAHs (polycyclic aromatic hydrocarbon molecules) may be traced by dust emission, and would make excellent targets for e^+ s to annihilate with because of their huge ‘effective charge number’, Z_{eff} , and therefore reaction cross section. PAHs show Z_{eff} values of up to 10^8 , so that their cumulative effect in the ISM may lead to reaction rates of $\sim 10\%$ of the dominating processes in the warm neutral and ionised medium, even though their number abundance is only 10^{-6} (Guessoum et al, 2010). It is apparent that the Milky Way dust map does not trace the 511 keV map, except again for the possible high latitude emission.

Particle acceleration and propagation:

Annihilation of e^+ s in flight (see Sec. 3, and, e.g., Beacom and Yüksel, 2006; Sizun et al, 2006), either through charge exchange or directly, may be traced by several processes that should show their paths of transport. Positrons should be bound to the large-scale magnetic field of the Galaxy, so that the synchrotron emission (e.g. at 408 MHz, Haslam et al, 1981) could show places where e^+ s annihilate. Likewise, bremsstrahlung (free-free emission, and N. Aghanim et al, 2016) could possibly show the catastrophic energy loss of e^+ s, being removed from the scheme due to annihilation in flight. Electron bremsstrahlung and e^+ bremsstrahlung are hardly distinguishable, so that the free-free emission map in Fig. 1 may show both particle populations. At very high energies, beyond 100 MeV, the Galactic emission is dominated by pion decay ($\pi^0 \rightarrow 2\gamma$, Bjorklund et al, 1950) as a result of high-energy cosmic-ray interactions with the dense ISM (e.g., Ackermann et al, 2013). Therefore, this emission might represent both, production site and destruction site of e^+ s. But also for pion decay, the bulge emission would be missing as seen in the Fermi/LAT image above 1 GeV in Fig. 1. At these photon energies, there is also no high-latitude component¹ and the emission

¹The Fermi Bubbles (e.g., Su et al, 2010) are high-latitude emission but confined to longitudes $-10^\circ \lesssim \ell \lesssim 10^\circ$.

is clustered around star-forming regions, dense molecular clouds, and spiral arms.

In-situ annihilation:

If the propagation of e^+ s is not ballistic (Sec. 3), i.e. not determined by collisional transport (Jean et al, 2009), they might be advected with the Galactic velocity field rather than diffusing several kpc. This may result in morphologies that would resemble the possible sources of e^+ s (Sec. 2), such as nucleosynthesis ejecta (e.g. shown as the 1.809 MeV map), X-ray binaries (XRBs; e.g. shown as the X-ray all-sky map from ROSAT), or, indeed, stars themselves through flares (traced by infrared and visible light, Bisnovaty-Kogan and Pozanenko, 2017). Especially in the latter case, the need for e^+ propagation in the ISM would be weakened as parts of the emission are entirely explained so that a different set of constraints will emerge. This may include only propagation inside the bulge, for example, and no channelling of e^+ s from the disk into the bulge (e.g., Higdon et al, 2009). For XRBs, a population of point-like sources would be expected for the 511 keV emission, or, after propagation, again an image similar to the HI, CO, or dust maps. The hot tenuous X-ray gas with temperatures above 1 MK is probably too thin for e^+ s to efficiently cool down and annihilate in large numbers (see, however, Sec. 3.2). The 1.809 MeV emission from ^{26}Al , a β^+ -decaying massive star nucleosynthesis product, shows potentially the negative image of HI, i.e. instead of the shell boundaries now the interiors. These cavities are filled with hot gas streaming away from the stellar groups into lower pressure regions (Krause et al, 2015). Again, e^+ s would start out at low densities and high temperatures, so that only after reaching the HI walls, they would annihilate, then in the vicinity of the sources. More information about the possible sources of Galactic e^+ s are presented in Sec. 2.

Statistical comparison:

The visual inspection of these maps with the physical arguments from spectroscopy should not be over-interpreted because the reconstruction of the 511 keV emission itself is biased by the assumptions of how a Galaxy may look like. Instead, one

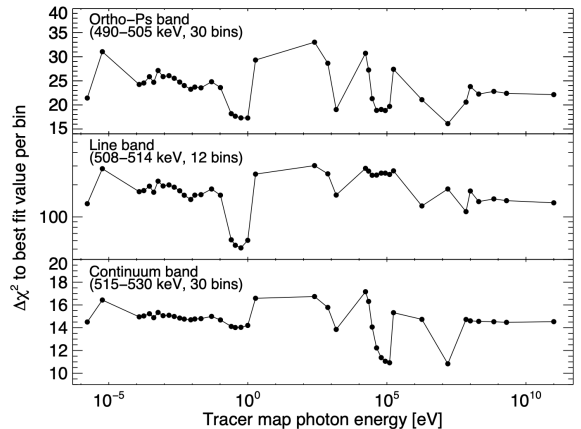


Fig. 3 Likelihood comparisons of different tracer maps as a function of photon energy in three bands, including the ortho-Ps continuum, the 511 keV line, and the diffuse Galactic continuum emission (Siebert, 2017).

can define an adequacy-of-fit criterion², $\Delta\chi^2 = -2 [\ln \mathcal{L}(\text{BG} + \text{SKY}) - \ln \mathcal{L}(\text{BG})]$. This may be interpreted as a relative measure, which template maps, either by wavelength or physical process, fit the raw data best. I want to stress, that this is not an absolute measure of how good the fit is, nor is this intended. Fig. 3, shows the $\Delta\chi^2$ -values as a function of tracer map photon energy for the ortho-Ps band, the 511 keV line band, and the continuum band above the e^+ -annihilation line (Siebert, 2017). It can be seen that the line and ortho-Ps behave similarly as a function of tracer map photon energy, except for the 10–200 keV range. This is understandable because the continuum emission above the line is nicely traced by X-ray sources as seen by the dip (improvement) in $\Delta\chi^2$ in the lower panel, and also impacts the emission below the line. The only all-sky maps that consistently show an improvement in $\Delta\chi^2$ for both 511 keV and ortho-Ps are the infrared maps below 1 eV (1.25–4.9 μm) from COBE/DIRBE. This improvement is not seen in the continuum band, so that it is prone to e^+ -annihilation.

This means that star light (and the zodiacal light, which has not been removed from the maps; see also Sec. 4.1) apparently traces annihilating e^+ s – not their presumed sources, nor the ISM. Stars may be both, the dominant sources and the natural sinks, of e^+ s in the Galaxy. In fact,

²This is not a goodness-of-fit criterion, since it is not statistically sound to judge a fit based on such a likelihood comparison.

contemporaneous to Siegert (2017), Bisnovatyi-Kogan and Pozanenko (2017) suggested flaring stars to be a major contributor to the Galactic 511 keV signal.

Such a template-fit analysis has also been performed by Knoedlseder et al (2005) to the 511 keV line, with only 1.5 yr of exposure in the Galaxy, resulting in similar conclusions that the emission might be related to the or an old stellar population (see also Siegert et al, 2022c). These types of analyses may appear odd for non- γ -ray astronomers, but because of the fact that we cannot directly (or only hardly) image the γ -ray sky leads us to such fundamental comparisons. Knödlseeder (1999) performed also a similar study for the origin of the 1.8 MeV line from decaying ^{26}Al , finding that the free-free emission at 53 GHz is correlating with the measurements from COMPTEL. This result was part of the solid proof that massive stars are indeed responsible for the observed ^{26}Al . The conjecture for the e^+ sources is ‘*the old stellar population*’, but what exactly this entails is not yet clear, since the interpretations are still versatile.

2 Positron sources

The general, straight-forward, question of the Positron Puzzle is ‘*Where do the positrons come from?*’, meaning, what are the sources to explain the amount that annihilates in the Milky Way. The list of potential candidate sources is large because nearly every astrophysical source can produce e^+ s either directly or through secondary interactions with the surroundings. Consequently, the actual problem is not *which* sources are responsible, but rather that *there* are too many possibilities³.

Another fundamental predicament of the Positron Puzzle is that it appears that its solution will only benefit the puzzle itself, then being solved. But the fact that nearly every astrophysical source indeed is able to produce (and annihilate) e^+ s may turn the 511 keV emission line into an independent astrophysical messenger, a tool to study other unsolved problems, a way to gain a perspective orthogonal to other measurable quantities. When the puzzle is solved, and it eventually turns out that many different astrophysical source types contribute to the Galactic

511 keV emission, a dedicated observatory may revolutionise our understanding in the multiple fields of astrophysics associated with it. In the following, I will summarise candidate sources and put them into the context of available observations to estimate their contribution, given measurement uncertainties and systematics from model assumptions. This is closely following Siegert (2017) but will be more concise. For completeness, I will briefly describe the particle physics processes that can lead to e^+ s.

2.1 Positron production mechanisms

β^+ -decay:

The most intuitive answer to the question where e^+ s could emerge from is the radioactive decay of isotopes with a proton excess. The generic equation for β^+ -decay is

$${}^A_Z\text{X} \xrightarrow{\tau_{A,X}} {}^A_{Z-1}\text{Y} + e^+ + \nu_e, \quad (2)$$

where a nucleus X with charge number Z and atomic number A decays within its lifetime of $\tau_{A,X}$ to another nucleus Y with reduced charge number $Z - 1$ but same atomic number by the emission of a e^+ and an electron-neutrino ν_e . For most nuclei, this is not the sole decay branch so that it is associated with a branching ratio, or equivalently, a probability p_{β^+} for this path. Astrophysically important nuclei can be associated to different objects (see Sec. 2.2) and are listed in Tab. 1 for completeness. It becomes clear that there is a variety of eleven orders of magnitude in lifetime of these relevant isotopes. This means e^+ s may either annihilate far away from their initial production sites, or they cool down quickly due to a possibly large density and find e^- s to recombine with at the position of their sources. A mixture of e^+ annihilation after propagation and in-situ would be the result.

Particle acceleration:

Positively charged mesons, such as pions and kaons, may also emit e^+ s, formally involving the same process of β^+ -decay. However, their production is only possible from the interaction of high-energy particles (including photons). Hadronic processes of the shape

$$p + p \longrightarrow \pi^{0,+,-} + X, \quad (3)$$

³Quoted after a lecture by G. K. Skinner.

Table 1 List of astrophysically important positron emitting nuclei, sorted by lifetime τ . The columns are the nucleus, its lifetime, the probability to emit a positron while decaying, possibly associated γ -ray emission from the daughter nucleus in units of MeV, and potential sources.

Nucleus	τ	p_{β^+}	E_γ	Sources
²⁶ Al	1.03 Myr	0.82	1.809	Massive stars, AGB stars, Supernovae
⁴⁴ Sc	81 yr ^a	0.94	1.157	Supernovae
⁴⁸ V ^d	23.1 yr	0.50	0.983, 1.312	Supernovae
²² Na	3.75 yr	0.90	1.275	Novae
⁵⁶ Co	111.4 d ^b	0.20	0.847, 1.238	Supernovae
⁵⁷ Ni ^d	2.14 d	0.43	0.127, 1.378, 1.920, 0.122 ^c , 0.136 ^c	Supernovae
¹⁸ F	2.64 h	0.97	–	Novae, Solar flares
⁵² Mn ^d	30.4 min	0.29	0.744, 0.936	Supernovae
¹¹ C ^d	29.3 min	>0.99	–	Cosmogenic (cosmic-ray interactions, spallation), Solar flares
¹³ N	14.4 min	>0.99	–	Novae, Earth atmosphere / lightning, Solar flares
¹⁵ O	2.94 min	>0.99	–	Novae, Earth atmosphere / lightning, Solar flares

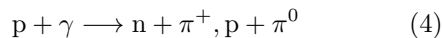
^a The nucleus ⁴⁴Sc only has a half-life time of 3.9 h and exists only as an intermediate step from the decay of ⁴⁴Ti. The relevant astrophysical timescale, for example for heating of supernova remnants, is that of the longer-living ⁴⁴Ti.

^b The nucleus ⁵⁶Co is the daughter product of the shorter-lived ⁵⁶Ni that is dominantly produced in supernovae. The relevant timescale here is again that of the longer-living ⁵⁶Co.

^c The γ -rays at 122 and 136 keV come from the daughter nucleus' decay, ⁵⁷Co \rightarrow ⁵⁷Fe which is no β^+ -decay, but the γ -rays might indicate that positrons have been emitted throughout the ⁵⁷Ni decay chain.

^d These isotopes have not been considered for the Positron Puzzle so far but may play a role.

and



are possible for threshold energies above ~ 280 MeV ($m_{\pi^0} \approx 135$ MeV, $m_{\pi^\pm} \approx 140$ MeV). For pp-interactions, Eq. (3), the production cross section rises logarithmically, reaches a plateau on the order of 1.4×10^{-25} cm² above ~ 1 TeV, and may rise afterwards again. Each π^+ produced will eventually lead to one e^+ , either directly or through the decay of an anti-muon. Because the pions produced will have large kinetic energies, the e^+ s will carry away this energy with Lorentz factors of 10^3 and more, but with a peak around 30–40 MeV (Murphy et al, 1987). Cosmic-ray production of secondary e^+ s will therefore lead to a very smeared out annihilation morphology as the e^+ s may be prone to large-scale propagation. For photo-pion production, Eq. (4), the arguments are similar, but the interaction cross section is reduced to $\sim 10^{-28}$ cm². Neutral pions have a dominant decay branch into two photons with 98.8%; the remaining $\sim 1.2\%$ allow for a decay into one photon and an e^-e^+ -pair. The effective production

rate of e^+ s from neutral pions is then about 1% of that of positively charged pions.

In addition to meson production, cosmic rays also lead to spallation reactions on ISM nuclei, thereby forming β^+ -unstable isotopes, such as ¹¹C.

Pair production:

Electron-positron pairs can be created by the interaction of high-energy photons in the electric field of a nucleus (or e^-), in a magnetic field, or by photon-photon pair production. The first reaction has a cross section proportional to Z^2 , and rises logarithmically with photon energy, showing typical values of $> 10^{-27}$ cm² above its threshold energy of 1.022 MeV (Maximon and Olsen, 1962). The second requires strong magnetic fields on the order of 10^{12} G to show an efficient photon to pair conversion. One cannot ascribe this process a cross section but rather an attenuation coefficient $\gtrsim 10^2$ cm⁻¹ for a magnetic field of 5×10^{12} G for photon energies above the threshold. Finally, photon-photon pair production has a maximum cross section close to the Thomson cross section of

$0.25\sigma_T = 1.66 \times 10^{-25} \text{ cm}^2$ at a centre of momentum energy of $4 \times 511 \text{ keV}$. The cross section is suppressed for energies near the threshold and decreases $\propto \gamma^{-1}$ for higher energies. Photon-photon absorption is important in the context of the mean free path, or, equivalently, the optical depth of very high-energy photons, for example from AGN or Galactic ‘pevatrons’: High-energy photons interact with the ubiquitous photon field of the cosmic microwave background (CMB) or the interstellar and intergalactic radiation field at infrared to optical wavelengths, leading to a cut-off in the TeV regime due to pair production. The rate of pair production in the intergalactic medium (IGM) due to photon-photon absorption from TeV emitting AGN has, to the knowledge of the author, not yet been calculated/estimated.

Svensson (1982a) studied the behaviour of a thermal proton-electron-positron-photon plasma, including the radiation mechanisms of bremsstrahlung, Inverse Compton (IC) scattering, pair annihilation and pair production through all the above-mentioned processes (except magnetic fields). This is particularly important in the case of black holes (BHs) with accretion disks, forming photon spectra up to MeV energies and therefore leading to an e^\pm atmosphere that may be carried away in an optically thin wind (Beloborodov, 1999). This pair-plasma would then annihilate according to its plasma temperature (Svensson, 1982b, 1983). It should be noted that pair-plasma annihilation will *not* produce a narrow 511 keV line unless the plasma temperature is particularly low. Instead, a blueshifted (Doppler-boosted), and broadened feature will emerge – searches for narrow annihilation lines in sources where pair-plasma would be expected will therefore always be negative even though pair-annihilation may have occurred.

Hawking radiation:

The evaporation of BHs due to Hawking radiation is the suggested cooling (and therefore mass loss) mechanism of these compact objects (e.g., Hawking, 1975). Hawking radiation is believed to be a quasi-thermal emission mechanism with a temperature $T_{\text{BH}} = 1.06 (10^{16} \text{ g}/M_{\text{BH}}) \text{ MeV}$, with M_{BH} being the mass of the BH, of not only photons but also particles – and therefore also e^\pm s. The kinetic energies of the particles will also have a blackbody

distribution so that a large variety of energies are possible according to the range of BH masses. Primordial black holes (PBHs, Hawking, 1971) may have masses on the order of $\gtrsim 4 \times 10^{17} \text{ g}$ (e.g., Siegert et al, 2022b; Bertheaud et al, 2022; Iguaz et al, 2021) which would result in average e^\pm energies of $\lesssim 100 \text{ keV}$, potentially not propagating far from the sources. The associated γ -ray signature would provide a smoking-gun evidence that PBHs may be responsible for the DM phenomenon as well as a major contributor to the annihilating e^\pm s. It should be noted that Hawking radiation is not proven by observations to actually exist.

Dark matter:

If DM is composed of beyond-standard-model particles, their decay (e.g., Hooper et al, 2004), annihilation (e.g., Boehm et al, 2004), or excitation (e.g., Finkbeiner and Weiner, 2007) might result in e^-e^+ -pairs. Depending on the actual particle candidate, i.e. its mass, e^\pm s carry away the parent particles’ rest mass energy as kinetic energy. Thus, e^\pm s may annihilate close to their production sites of light DM particles, leading to a 511 keV emission reminiscent of a DM halo, or far away because they diffuse over large distances from GeV–TeV mass scale WIMPs. In the latter case, the annihilation branch into massive quark-antiquark pairs is dominating over e^-e^+ -pairs (Jungman et al, 1996). However, the intermediate formation of charged mesons will eventually lead to e^\pm s, and potentially more than one per WIMP co-annihilation. It should also be noted here that there is no observational evidence of particle DM.

2.2 Astrophysical sources

Given the production mechanisms, Sec. 2.1, astrophysical sources can be associated, and, if observations are available, e^\pm s from individual candidate populations can be budgetised. Such an approach does not take into account the possible propagation of e^\pm s (Sec. 3) and shows that the puzzle is indeed either under- or over-explaining the annihilation rate in the Milky Way. Tab. 2 summarises the rates at which candidate populations (see following paragraphs) produce e^\pm s, including uncertainties from measurements as well as systematics from unknown population sizes, for example.

Source	Galaxy	Bulge	Disk
²⁶ Al	3.4 ± 0.1	0.35 ± 0.01	3.0 ± 0.1
⁴⁴ Ti	2.2 ± 0.3	0.22 ± 0.03	1.9 ± 0.3
⁵⁶ Ni	19 ⁺¹¹⁹ ₋₁₉	4.6 ⁺²⁹ _{-4.6}	14 ⁺⁹⁰ ₋₁₄
γγ	27 ⁺²⁹ ₋₂₇	8.9 ^{+9.5} _{-8.9}	18 ⁺¹⁹ ₋₁₈
∑ Sources	51 ⁺¹²² ₋₃₃	14 ⁺³⁰ ₋₁₀	37 ⁺⁹² ₋₂₃
Target Rate	49 ± 15	18.0 ± 0.2	31 ± 15
	Galaxy %	Bulge %	Disk %
²⁶ Al	7 ± 2	1.9 ± 0.2	10 ± 5
⁴⁴ Ti	4 ± 2	1.2 ± 0.2	6 ± 3
⁵⁶ Ni	39 ⁺²⁴³ ₋₃₉	27 ⁺¹⁶⁰ ₋₂₇	47 ⁺²⁹¹ ₋₄₇
γγ	55 ⁺⁶¹ ₋₅₅	49 ⁺⁵³ ₋₄₉	57 ⁺⁶⁷ ₋₅₇
∑ Sources	105 ⁺²⁵¹ ₋₆₇	78 ⁺¹⁶⁹ ₋₅₆	120 ⁺³⁰⁰ ₋₇₄
Target %	100 ± 31	100 ± 11	100 ± 48

Table 2 Comparison between measured e⁺s annihilation and production rate (top, in units of 10⁴² e⁺ s⁻¹) in the Milky Way. The contributions in per cent (bottom) to bulge and disk have been estimated from the ccSNe rates in the case of ²⁶Al and ⁴⁴Ti (10% bulge, 90% disk), from the SNe Ia rate in the case of ⁵⁶Ni (25% bulge, 75% disk), and from the stellar distribution in the case of γγ (33.3% bulge, 66.7% disk). For details, see Siegert (2017).

Massive stars and core-collapse supernovae:

Through massive star winds and their ultimate core-collapse supernovae (ccSNe), the ISM is enriched by freshly produced elements. For the production of e⁺s, the most important isotopes in stellar evolution are probably ²⁶Al, ⁴⁴Ti, and ⁵⁶Co. To a lesser extent also ⁵⁷Ni, ⁵²Mn, and ⁴⁸V may play a role, but have so far not been considered in the context of the Positron Puzzle, probably because of their small yields and shorter lifetimes (see, however, Panther et al, 2021). The e⁺-production rate follows directly from the radioactive decay law: If a mass M_i of radioactive, β⁺-unstable, isotope i is produced, the number of particles that decay per time is $N_i(t) = \frac{M_i}{m_i} p_i e^{-t/\tau_i}$, with m_i being the isotope mass, τ_i its lifetime, and p_i the probability of undergoing e⁺-emission (branching ratio). The e⁺-production rate, $\dot{N}_+(t)$, from isotope i is then

$$\dot{N}_i^+(t) = -\frac{dN_i(t)}{dt} = \frac{M_i p_i}{m_i \tau_i} e^{-t/\tau_i} = \frac{N_{0,i}^+}{\tau_i} e^{-t/\tau_i}. \quad (5)$$

It should be noted here – and is true for most other production sites – that the production rate, \dot{N}_+ , is *not* (necessarily) the annihilation rate, \dot{N}_\pm . Most

e⁺s are produced at relativistic energies and supposedly propagate in the ISM on Myr timescales until they annihilate, which makes it difficult to judge whether the 511 keV phenomenon is actually a steady state. In this context, also the escape of e⁺s from the Galaxy should be considered as they would be lost for current observational techniques⁴, even if they do annihilate in the IGM, for example. This means that the e⁺-production rate in the Milky Way may be larger or smaller than the measured e⁺-annihilation rate.

The advantage of a nucleosynthesis origin of e⁺s in the Galaxy is that we can directly measure the mass of ejecta, given we have a 3D geometrical model of the Galaxy and the γ-ray opacity of SN remnants as a function of time. Because each nucleus can only decay once, and if the possible γ-ray emission from daughter nuclei can be measured, we obtain a generic luminosity per isotope per solar mass, $L_\odot^i = p_i \dot{N}_i$, which directly

⁴Coded-mask telescopes, such as the currently best telescope to observe the 511 keV emission, INTEGRAL/SPI, cannot, or only hardly, observe isotropic emission as they rely on the contrast between emission and no emission to distinguish the instrumental background from the total signal. Shallow gradients in the morphology are also difficult to reliably detect with coded aperture masks (Siegert et al, 2022d)

converts to a e^+ -production rate, given Eq. (5):

$$\dot{N}_i^+ = 3.8 \times 10^{43} \frac{p_i}{A_i} \left(\frac{\tau_i}{\text{Myr}} \right)^{-1} \left(\frac{M_i}{M_\odot} \right) e^+ \text{ s}^{-1}, \quad (6)$$

where A_i is the nucleon number of isotope i .

For example, given the estimate of $2.8 M_\odot$ of ^{26}Al in the Milky Way (Siegert, 2017; Pleintinger, 2020), and a probability for β^+ -decay of ^{26}Al of $p_{26} = 82\%$, we obtain a production rate⁵ of $3.2 \times 10^{42} e^+ \text{ s}^{-1}$. These are at most 10% of the total annihilate rate in the Milky Way, which means that ^{26}Al alone cannot explain the measured 511 keV line, unless there was a star burst from which the e^+ s are still annihilating now (e.g., Prantzos et al, 2011; Alexis et al, 2014).

Considering the shorter-lived isotopes, such as ^{44}Ti , for example, we have to rely on the only direct measurement of ^{44}Ti in the Milky Way so far, the SN remnant Cassiopeia A (Cas A), to estimate the production rate. Assuming all e^+ s from ^{44}Ti to escape from the remnant, the total number produced is given by $N_{0,44}^+$, and the total production rate by the SN rate in the Milky Way, R_{SN} , as

$$\dot{N}_{\text{SN},44}^+ = N_{0,44}^+ R_{\text{SN}}. \quad (7)$$

With a ^{44}Ti ejecta mass produced in Cas A to be around $10^{-4} M_\odot$ (e.g., Renaud et al, 2006; Martin and Vink, 2008; Iyudin et al, 1997; Siegert et al, 2015; Weinberger et al, 2020), and a branching ratio of 0.94, we get a total number of e^+ s produced of $2.6 \times 10^{51} e^+$. With a ccSN-rate of $R_{\text{SN}} = 2/(100 \text{ yr})$ (e.g., Diehl et al, 2006), the ^{44}Ti e^+ -production from ccSNe in the Milky Way is about $1.6 \times 10^{42} e^+ \text{ s}^{-1}$ – of the same order of magnitude as ^{26}Al . It should be noted that this may even be considered an upper bound of the production rate from ^{44}Ti because the yield per ccSN may indeed be lower and Cas A exceptional, and because it has been shown in the case of SN1987A that e^+ s are responsible for heating the remnant at early times (Seitenzahl et al, 2014). However, also thermonuclear SNe produce ^{44}Ti , which enhances the ^{44}Ti e^+ -production rate by about a factor of 2.

Type Ia supernovae:

The case for type Ia supernovae (SNe Ia) in the Galaxy is even more insecure: While the amount

of ^{56}Ni produced in SNe Ia is about $0.1\text{--}1.0 M_\odot$ (from Arnett's rule, Arnett, 1982; Stritzinger et al, 2006), and the branching ratio for β^+ -decay of the daughter nucleus ^{56}Co about 20%, the escape fraction of e^+ s from the expanding remnant is very uncertain. Because ^{56}Ni and ^{56}Co have lifetimes of only 8 d and 111 d, respectively, it can be expected that most e^+ s do not manage to escape into the ISM but rather annihilate in situ. Milne et al (1999) showed that the escape of e^+ s is probably on the order of 3%, as estimated from the late lightcurves of a sample of SNe Ia. The only direct measurement of the ^{56}Ni mass from a SN Ia is from SN2014J, estimating $0.4\text{--}0.6 M_\odot$ (Churazov et al, 2014; Diehl et al, 2015). The data suggest that there indeed is a broadened 511 keV line, but the flux uncertainties make it difficult to reliably estimate a e^+ escape fraction. At face value, the average escape fraction η from SN2014J during the half-year observation time is $\eta = 0.06_{-0.06}^{+0.33}$ (Siegert, 2017). Therefore, similar to the ^{44}Ti case, the e^+ -production rate from ^{56}Ni in SNe Ia is

$$\dot{N}_{\text{SN},56}^+ = N_{0,56}^+ \eta R_{\text{SNIa}}. \quad (8)$$

Using the γ -ray measurements from SN2014J and an estimated SNe Ia rate in Milky Way of 0.25/century, the ^{56}Ni e^+ -production rate is $(2_{-2}^{+12}) \times 10^{43} e^+ \text{ s}^{-1}$. At a face value of $\eta = 0.03$ and a canonical ^{56}Ni ejecta mass of $0.5 M_\odot$, the production rate would be $5.1 \times 10^{42} e^+ \text{ s}^{-1}$ – again of similar magnitude than the previous two nucleosynthetic e^+ origins. It is clear that e^+ s from SNe Ia may either explain the complete signal, none of it, or even more than is measured.

Classical novae:

Classical novae (CNe) have never been detected in MeV γ -rays, so that a direct estimate of the important ejecta masses has not been possible so far. In CNe, two contributions may be of interest, either the '511 keV flash' from very short-lived β^+ -unstable nuclei, such as ^{18}F (2.64 h) or ^{13}N (14.4 min), or from the longer-lived ^{22}Na (3.75 yr). While the latter is dominantly only produced in ONE novae, the former are expected in all types of CNe. Models (e.g., Gomez-Gomar et al, 1998; José and Hernanz, 1998; Hernanz et al, 2000; José et al, 2001; Hernanz and José, 2006; Hernanz, 2014) suggest a γ -ray flash at the onset of the CN – the explosion on the surface of the white

⁵Detailed modelling then provides the numbers in Tab. 2.

dwarf –, several days before the optical emission maximum. The exact time is unknown, but the flux from the e^+ s annihilating directly on the surface is on the order of 10^{-3} – 10^{-2} $\text{ph cm}^{-2} \text{s}^{-1}$ at 511 keV for a distance of 1 kpc for a duration of about 1 h. This would be easily detectable by current γ -ray telescopes, but has never been observed. This might, in fact, cast doubts on the strength of the 511 keV line from the very-short-lived isotopes, and it has been suggested by Leung and Siebert (2022) that the flux would be heavily suppressed because the initial ejecta velocity could be much smaller than expected, so that the opacity stays at higher values at early times. With a flux of 10^{-9} – 10^{-8} $\text{ph cm}^{-2} \text{s}^{-1}$ at 511 keV, these lines could never be detected with current instrumentation. In any case, these e^+ s would most probably fall into the in-situ annihilation case unless they also escape.

For ^{22}Na , we have to rely so far on stellar evolution models and nucleosynthesis calculations to estimate the contribution of CNe to the remaining Positron Puzzle. While 1/3 of all CNe are considered ONe novae, and the CNe rate in the Milky Way is about 20 – 60 yr^{-1} (Shafter, 2017), the expected contribution of ^{22}Na e^+ s is $< 3 \times 10^{41} \text{ e}^+ \text{ s}^{-1}$. Measurements only find an upper limit on the cumulative flux of ^{22}Na γ -rays at 1275 keV in the Milky Way of $< 2 \times 10^{-7} \text{ M}_\odot$ per nova, which converts to an upper bound of the e^+ -production rate of $< 5 \times 10^{42} \text{ e}^+ \text{ s}^{-1}$ (Siebert et al, 2021c) – about ten times higher than the theoretical expectation. CNe make at most 10% of the total annihilation rate in the Milky Way if a steady state is assumed, and it is suggested from yield models that their contribution is even less than 1%. It should be noted here that the contribution of CNe to Galactic ^{26}Al is still debated, so that the e^+ -budget for massive stars might be decreased and for CNe increased, but will not change in total.

Other nucleosynthesis origins:

In the above considerations, we only took into account the standard classes of objects. Rare but strong events (or similarly weak but frequent events) may contribute significantly to the production of e^+ s in the Galaxy. There are no direct

measurements on which we could base our estimates on, so that here, we only list these objects as possible additions(!) to the total production rate.

Hypernovae, for example, which may be related to pair-instability supernovae, could produce 20 – 40 M_\odot of ^{56}Ni , as suggested from SN2006gy in NGC1260 (Smith et al, 2007). If such an event happened every 1000 yr, the Milky Way annihilation rate could be sustained by hypernovae alone, even with an escape fraction of 1%. However, the hypernova interpretation has been contested with other scenarios, for example as interactions with the ISM would strongly decrease the ^{56}Ni mass (e.g., Jerkstrand et al, 2020; Fox et al, 2015).

Another scenario which may explain all the e^+ s in the Galaxy required to meet its annihilation rate is by Crocker et al (2017). In a similar fashion as the superluminous supernovae, a rare type of SN Ia, SN1991bg, may produce large amounts of ^{44}Ti . In this scenario, a low-mass He white dwarf merges with a low-mass CO white dwarf to produce a subluminous SN Ia. Because of the large amounts of He available, the yields of ^{44}Ti may be as high as 0.03 M_\odot , 10^2 – 10^4 times more than expected (and measured) for ‘normal’ ccSNe and SNe Ia. With a rate of these objects of 1 every 500 yr, averaging to about 15% of all SNe Ia to be of SN1991bg-type, the total production rate would be on the order of $5 \times 10^{43} \text{ e}^+ \text{ s}^{-1}$. There is indeed evidence that these objects produce Ti as measured from absorption spectra around 420 nm (see also Higdon et al, 2009).

Compact objects:

In compact objects, i.e. in particular neutron stars (NSs) and BHs, pair production by photon-photon interactions is probably the dominant e^+ production channel. Despite the fact that the production cross section of photon-photon-pair-production is calculated as

$$\sigma_{\text{pair}} = \frac{3\sigma_T}{16}(1-\beta^2) \left[(3-\beta^2) \ln \left(\frac{1+\beta}{1-\beta} \right) - 2\beta(2-\beta)^2 \right], \quad (9)$$

which has a maximum at $\beta = 0.7$ for $\sigma_{\text{pair}}^{\text{max}} \approx 1.7 \times 10^{-25} \text{ cm}^2$, i.e. on the same order of magnitude as the Thomson cross section, photon-photon-pair-production has never been unambiguously observed in laboratory experiments. Due to the high densities of high-energy photons needed, this

process is only efficient when the optical depth $\tau_{\gamma\gamma} = n_{\gamma}\sigma_{\text{pair}}x$, with x being the physical size of the emitting objects, is larger than unity. This can be expressed in terms of the so-called compactness parameter l , as

$$l \equiv \frac{L\sigma_T}{rm_e c^3} = 2\pi \left(\frac{m_p}{m_e}\right) \left(\frac{L}{L_E}\right) \left(\frac{r_S}{r}\right), \quad (10)$$

where L_E is the Eddington luminosity and r_S is the Schwarzschild radius of the source, both being a function of the object's mass (Lightman and Zdziarski, 1987). For efficient pair production, $l \gtrsim 10$, which means that for small objects and/or large luminosities, *pair production is inevitable*. Such compactness values are naturally possible for BHs, NSs, and to a smaller extent also WDs.

X-ray binaries (XRBs), and in particular low-mass XRBs (LMXRBs) were discussed in terms of the ‘Positron Puzzle’ shortly after the launch of INTEGRAL (Prantzos, 2004). They raised even more attention because their spatial distribution appeared similar to that of the 511 keV image with an enhancement towards negative longitudes (Weidenspointner et al, 2008). It turned out that the INTEGRAL/SPI measurements at this point in time were not representative of the full Galaxy so that a claim considering an XRB-origin due to the similar spatial distribution is flawed. Nevertheless are XRBs promising e^+ -producers as the annihilation of the pair-plasma that is produced in these objects has supposedly been measured in three different objects, the ‘Great Annihilator’ (1E1740.7-2942, Bouchet et al, 1991), Nova Musca (GRS1124-68, Goldwurm et al, 1992; Sunyaev et al, 1991), and V404 Cygni (GS2023+338, Siebert et al, 2016a). All of these measurements are contentious because independent analyses could not confirm the, most of time, weak signals.

The models for pair production in XRBs (e.g., Beloborodov, 1999), their annihilation as plasma (e.g., Svensson, 1983), and possible escape into the ISM (e.g., Beloborodov, 1999) result in order of magnitude estimates for the total population of compact objects in the Galaxy. Given the measurements of V404 Cygni, for example, we can estimate a e^+ -production rate of $(1.1 \pm 0.3) \times 10^{42} e^+ s^{-1}$. Note that even if the pair-plasma annihilation feature in the spectra

are doubted, the MeV spectrum extends significantly above 511 keV, so that pair production is inevitable (Svensson, 1987; Maciolek-Niedzwiecki et al, 1995). In the case of V404 Cygni with a luminosity of 20% Eddington (Rodriguez et al, 2015), the photon-photon absorption has to take place within $\approx 10r_S$. This leads to an efficient absorption of γ -rays as they can interact with the more numerous X-rays, which leads to a suppression of photon energies $\gg m_e c^2$. Estimates of the GeV flux of $< 10^{-6} \text{ ph cm}^{-2} \text{ s}^{-1}$ corroborate this scenario (Siebert et al, 2016a; Harvey et al, 2021).

Assuming a power-law-shaped seed spectrum (Beloborodov, 1999), the luminosity that potentially contributes to the e^+ -production in XRBs can be estimated. Assuming further that the γ -ray measurements in V404 Cygni are indeed pair-plasma-annihilations, the escape fraction of e^+ s can be estimated to be $\eta_{\gamma\gamma} = (60 \pm 20)\%$. The theoretical value should be at most 20%; other analyses of the same source would suggest an escape close to 100% (Roques et al, 2015; Jourdain et al, 2017). These values are all of the same order of magnitude, and a canonical production rate per XRB in outburst in the Milky Way can be given as $\dot{N}_{\gamma\gamma, \text{XRB}}^+ = 10^{42} e^+ s^{-1}$ – corroborated by measurements.

To estimate the total contribution of micro-quasars and other XRBs to the e^+ -production in the Galaxy, one needs to estimate the duty cycle of such sources, and the total number of objects from population synthesis calculations (Guessoum et al, 2006). The duty cycle ϵ_{XRB} may be on the order of 10^{-3} – 10^{-2} , since per year, about one XRB is found in outburst for about 1–10 d. The total number of XRBs in the Galaxy may be in the range of $N_{\text{XRB}} \approx 10^4$ as suggested by several works (e.g., Romani, 1992; Portegies Zwart et al, 1997; Bandyopadhyay et al, 2009). The total number of e^+ s from the population of XRBs in the Milky Way is then

$$\dot{N}_{\gamma\gamma}^+ = N_{\text{XRB}} \epsilon_{\text{XRB}} \dot{N}_{\gamma\gamma, \text{XRB}}^+ = (3 \pm 3) \times 10^{43} e^+ s^{-1}. \quad (11)$$

Again, at face value, and motivated by observations, XRBs may explain the entire annihilation rate in the Galaxy if a steady state is assumed. However because their escape is uncertain, the seed spectrum is uncertain, the duty cycle is uncertain, and the number of objects in the Galaxy is uncertain, the population of XRBs may

also contribute insignificant amounts of e^+ s for the Positron Puzzle.

Pulsars:

The contribution from pulsars, i.e. pair production in magnetic fields, can only be estimated theoretically, or by considering the measurements of cosmic-ray e^+ s in the Solar System. Based on geometrical models, the e^+ -production rate by pulsars can be estimated as

$$\dot{N}_{B\gamma}^+ \approx 2.8 \times 10^{37} \left(\frac{B}{10^{12} \text{ G}} \right)^{10/7} \left(\frac{P}{\text{s}} \right)^{-8/21} e^+ \text{ s}^{-1}, \quad (12)$$

where B is the dipole magnetic field strength of the pulsar and P its rotation period (Cheng et al, 1986; Zhang and Cheng, 1997). Given the population of pulsars in the Milky Way, including normal ones, millisecond pulsars, and magnetars⁶, a total production rate of $\dot{N}_{\text{Pulsars}}^+ \approx 5 \times 10^{42} e^+ \text{ s}^{-1}$ can be estimated.

Interestingly, Eq. (12) can be used to estimate the distance a single pulsar must have to explain the entire 511 keV flux from the direction of the Galactic bulge: In this ‘one neutron star’ solution, the 511 keV flux of $(1-3) \times 10^{-3} \text{ ph cm}^{-2} \text{ s}^{-1}$ from the entire Milky Way is used and placed at a distance d away from the Solar System. Clearly, this estimate suggests that all e^+ s slow down in a way that the 511 keV morphology is recovered, which may not be the case, but the scenario is easily scalable. Assuming that the pulsar e^+ -production rate and observed flux are a steady state, the resulting plane of $F_{511}-d$ can be found in Fig. 4. Given typical numbers for normal, millisecond pulsars (MSPs), and highly magnetised NSs (magnetars), the entire measured 511 keV line flux can be explained by a single magnetar at a distance of 100–200 pc. Smaller fluxes may still be explained by regular pulsars at such a distance.

It is intriguing that the high-energy e^+ -excess from cosmic-ray measurements with AMS-02 also suggests a nearby ($\lesssim 250 \text{ pc}$) and young ($\approx 0.1 \text{ Myr}$) pulsar (Aharonian et al, 1995; Faherty et al, 2007). Indeed, including the Geminga pulsar significantly improves the description of the AMS-02 data (Yin et al, 2013; Di Mauro et al, 2014).

⁶For millisecond pulsars and magnetars, the dipole assumptions may not be valid anymore.

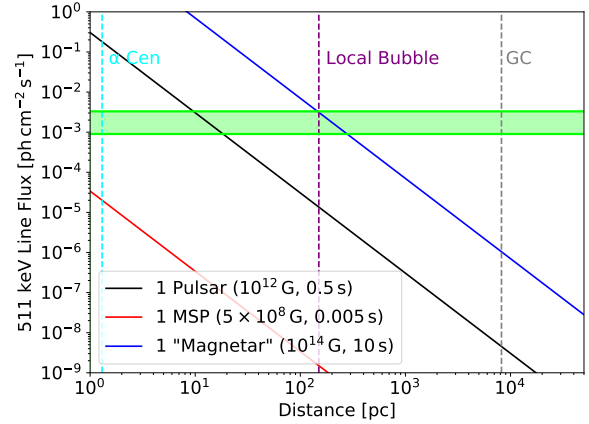


Fig. 4 The ‘one neutron star solution’ of the Positron Puzzle: The flux of the Galactic 511 keV line (green band) placed at a distance of 100–200 pc can be explained by the production rate of a single magnetar (blue line, magnetic field 10^{14} G). Smaller fluxes, such as the $8 \times 10^{-5} \text{ ph cm}^{-2} \text{ s}^{-1}$ from the direction of the Galactic centre, may be explained by a single pulsar with a magnetic field of $\sim 10^{12} \text{ G}$.

The question emerges: ‘why not relating the two problems?’ The canonical answer to this question is that ‘the kinetic energies of the e^+ s would be too large.’ As I will argue in Sec. 3, such a statement may be flawed, first in terms of astrophysics, and second in terms of analysis. This dogma reappears also in the case of general cosmic-ray e^+ -production as well in the case of DM.

Supermassive black holes – the case of Sgr A*:

Similar to stellar mass black holes, supermassive black holes (SMBHs) with masses of 10^6 to $10^9 M_{\odot}$ could also produce e^-e^+ -pairs in the vicinity of their event horizons, near the hot inner accretion disk, above in their coronae, or in relativistic jets. For the SMBH in the centre of the Milky Way, Sgr A* (e.g. Genzel et al, 2003; Ghez et al, 2004), the accretion history is the most important factor in the context of the ‘Positron Puzzle’. In the quiescent state it is now, its accretion rate is on the order of 10^{-8} – $10^{-6} M_{\odot} \text{ yr}^{-1}$ (Baganoff et al, 2003). If Sgr A* had phases of higher activity, an accretion rate of up to $10^{-4} M_{\odot} \text{ yr}^{-1}$ might have been possible, which would have increased the inner accretion disk temperature up to 10^{11} K (Totani et al, 2006). Such a large accretion rate may be due to tidal disruption events of low-mass stars (Cheng et al, 2007), massive star winds

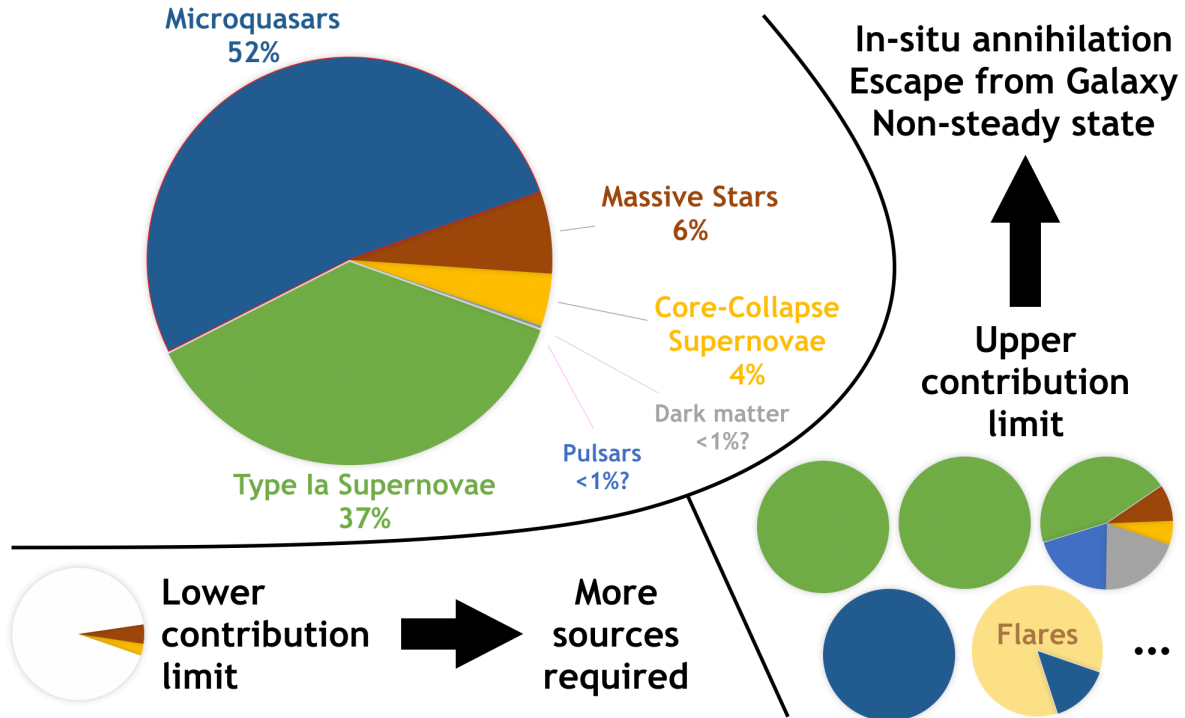


Fig. 5 Positron production rate in the Milky Way. *Top left:* About 105 % of the e^+ s seen to annihilate are composed of measured β^+ -emitters (SNe Ia, massive stars, ccSNe, in total $\approx 47\%$) and microquasars in outburst ($\approx 52\%$). DM, pulsars, cosmic-ray secondaries, and in general e^+ s sources with Lorentz factors $\gamma \gtrsim 100$, might not contribute at all to the 511 keV line. *Bottom left and right:* Taking into account the measurement uncertainties in both production and annihilation, as well as the uncertainties in population sizes and additional model variants, may either result in at most 10 % production vs. annihilation so that more sources would be required, or more than 500 % production vs. annihilation which might indicate a non-steady-state scenario, significant escape from the Galaxy, or dominant in-situ annihilation (Siegert, 2017).

(Quataert, 2004), or from the ionised halo surrounding the SMBH (Totani et al, 2006). In either case, this may be enough to produce thermal MeV γ -rays, which in turn would create e^-e^+ pairs, but on a much shorter timescale than the annihilation is expected to happen.

The model by Totani et al (2006) suggests that Sgr A* alone could provide a 511 keV line flux on the order of 10^{-3} ph cm $^{-2}$ s $^{-1}$ if the accretion rate about 300 yr ago was 10^3 – 10^4 times higher than now. Another possibility could be periodic tidal disruption events with a timescale of 100 kyr (Cheng et al, 2007), or episodic interruptions of e^+ production in Sgr A* due to quenching from nearby SN explosions (Totani et al, 2006). Steady production of e^+ s due to proton-proton interactions in the vicinity of Sgr A* would then occur on shorter timescales than in the ISM, for example. The e^+ s might then diffuse outwards and fill up the bulge, but which has been shown to come with energetic constraints (Panther et al, 2018a).

In any case, the measured point-like source in the centre of the Galaxy (Skinner et al, 2014; Siegert et al, 2016b) may be due to e^+ s from Sgr A*, but the narrow 511 keV line instead of the expected pair-plasma feature for BHs would point to the enhanced gas density in the CMZ rather than the SMBH itself.

Cosmic ray secondaries and γ -ray albedo of the Solar System:

Cosmic rays that have been accelerated by SN remnants, for example, reaching up to $\approx 10^{15}$ eV, in addition to ultra-high-energy cosmic rays up to 10^{21} eV, can lead to secondary e^+ s as a result of high-energy collision. Porter et al (2008) estimated the secondary e^+ -production from cosmic rays by propagation models, taking into account energy losses, diffusion, and escape, to be between $(1-2) \times 10^{42}$ e^+ s $^{-1}$. Again, the contribution is on the order of a few percent of the total measured annihilation rate, but this time with large

kinetic energies, peaking around 30–40 MeV and extending to several GeV–TeV (Murphy et al, 1987). Such e^+ s may again be ‘too fast’ to explain the Galactic 511 keV signal for which eV-scale particles are required (see Sec. 3.2).

In addition to secondary e^+ -production of cosmic rays with interstellar gas and molecular clouds, primary cosmic rays also interact with solid bodies in the Solar System. Moskalenko and Porter (2007) and Moskalenko et al (2008) calculated the γ -ray spectrum of cosmic rays interacting with small Solar System bodies as well as the Earth Moon. The 511 keV line from rapid energy losses of secondary e^+ s in the rock material followed by direct annihilation is on the order of 2×10^{-4} ph cm⁻² s⁻¹ distributed along the ecliptic. This emission would in fact be time variable as the asteroids and trojans move significantly with respect to the Earth orbit around the Sun, so that different hot spots may emerge at different times (Siegert 2023, in prep.; see also Sec. 4.1). This might also be the reason why this emission component has so far not been detected. The Moon would show a 511 keV line on the order of 2×10^{-5} ph cm⁻² s⁻¹, and would make a significant foreground component if observed with large-field-of-view instruments. The quiet Sun, Earth itself and planets are also plausible 511 keV contributors from cosmic-ray bombardment.

Dark matter:

Dark matter density profiles to explain the observed phenomena of flat rotation curves, structure formation, and high mass-to-light ratios in dwarf galaxies, are reminiscent of the 511 keV morphology, without the disk. It can be shown that an NFW profile squared, as suggested from the co-annihilation of DM particles, can replace the three bulge components to describe the γ -ray data statistically (Skinner et al, 2014). There are, however, more astrophysically relevant templates that fit the data better (Siegert et al, 2021b), such as a combination of a (smoothed) infrared bulge (Freudenreich, 1998) plus a (smoothed) nuclear stellar cluster (Launhardt et al, 2002). If DM particles are on the GeV–TeV mass scale, multiple e^- s and e^+ s are emitted from their annihilation, resulting in a strong contribution to the IC spectrum in the Milky Way at MeV energies. These DM annihilation products have also been invoked

to explain the cosmic-ray e^+ -excess as an alternative to the nearby pulsar scenario (see review by, e.g., Serpico, 2011).

Associating the 511 keV line in the Milky Way to DM products is difficult because, as shown above, the contribution of many other sources would produce an irreducible fore- and background. Other galaxies, and in particular dwarf galaxies, may provide better targets to distinguish 511 keV models. Siegert et al (2016c) found a hint at 511 keV from the dwarf galaxy Reticulum II (Ret II) – contemporary to a hint at GeV energies (Geringer-Sameth et al, 2015). With increased exposure and refined data analysis, it was shown that this signal was a fluke. It was further argued by Siegert et al (2016c) that the DM contribution to the 511 keV signal in the Milky Way, based on the serendipitous signal from Ret II, would be at most 1%. Because the signal in Ret II may in fact be smaller than what has been measured before, and assuming no astrophysical background in Ret II to the 511 keV signal, the previous statement only holds if the DM e^+ s cool down quickly and annihilate fast without escaping to the IGM. Since the only loss would be due to IC scattering, the escape is probably inevitable, but would also show a strong contribution again at the MeV continuum.

If the DM particles, instead, are of MeV scale, the behaviours would be similar to that of nucleosynthesis and pair production origins. As will be discussed in Sec. 3, the propagation may either be ballistic (collisional) for which large distances could be travelled within a typical e^+ lifetime of 0.1–10 Myr in the ISM, or advective, following the Galactic gas flow with diffusion length scales on the order of 1 pc due to the small gyro-radii. MeV e^+ s may either emerge from particle DM or PBHs in the mass range of 10^{14} – 10^{17} g.

It is difficult to estimate relevant parameters, such as DM annihilation cross sections, from the measurements of the Milky Way alone. Attempts that claim to be ‘conservative’ and overplot the maximum possible spectrum at 511 keV from a population of DM particles in the Milky Way are not useful: Gamma-ray data analyses rely on model expectations versus measured count rates – a model comparison that uses already-extracted fluxes, i.e. values that already assumed a model (e.g. a power-law per energy bin), is flawed and

can lead to much *tighter* limits than the anticipated ‘conservative’ approach. Instead, all models that are required to explain the data should be included, so that their intrinsic degeneracy given the measurement methods, are taken care of. The uncertainties per model component can and will be much larger than the sum of all components because of the covariance between components. This means that overplotting DM models on total spectra of the Milky Way in the keV–TeV range is wrong and upper limits from such attempts are not meaningful.

In addition to DM annihilation to pairs, also their internal bremsstrahlung should be taken into account, their IC scattering off the interstellar radiation field and the CMB, the annihilation in flight of e^+ s, and the final annihilation resulting in the 511 keV line and ortho-Ps spectrum. The renewed analyses of Ret II is doing that (except for IC) and determines upper bounds on DM decay and annihilation cross sections as well as PBH mass limits. The velocity averaged cross section has an upper bound of $\langle\sigma v\rangle \lesssim 5 \times 10^{-28} (m_{\text{DM}}/\text{MeV})^{2.5} \text{ cm}^3 \text{ s}^{-1}$ and excludes PBH masses to make the gross of DM of $\lesssim 8 \times 10^{15} \text{ g}$ (Siegert et al, 2021a). The particle DM limits are among the strongest compared to current literature (see also Laha et al, 2020; Slatyer, 2016; Ng et al, 2019, for more limits). The strongest PBH evaporation limit is derived from the Cosmic Gamma-ray Background (CGB) including the redshift-integrated 511 keV contribution as well as the isotropic DM halo component of the Milky Way by Iguaz et al (2021), and from the DM halo of the Milky Way itself, taking into account any possible foreground to obtain a DM-only spectrum by Berteaud et al (2022). From BH evaporation, PBH masses of $\lesssim 4 \times 10^{17} \text{ g}$ are excluded to account for 100% of the DM mass in the Milky Way. To exclude higher masses, the keV emission in the Milky Way must be studied as also fewer e^+ s will be produced.

Stellar flares:

From RHESSI, SMM, Fermi/GBM, and INTEGRAL measurements, for example, we know that solar flares can lead to a strong 511 keV line and ortho-Ps continuum due to particle acceleration and subsequent production of pions

and their decay. Whether the line is ubiquitous for all flare strengths and for all stars is a plausible, yet unproven assumption. From Kepler and TESS measurements (e.g., Shibayama et al, 2013), it is known that also other stars flare in a similar fashion as the Sun, with a flare-frequency-energy-distribution of $\frac{dN}{dE dt} \approx 10^{-29} \left(\frac{E}{10^{30} \text{ erg}}\right)^{-1.8} \text{ erg}^{-1} \text{ yr}^{-1}$. From the rare X-class flares with energies above 10^{31} erg , RHESSI could measure high-resolution spectra in the MeV range, finding also nuclear excitation lines in addition to the strong neutron capture line at 2.2 MeV and the e^+ -annihilation line at 511 keV (Lin et al, 2002). Murphy et al (2005), Murphy et al (2014), and Share et al (2004) studied the annihilation of e^+ s in the solar atmosphere during flares in great detail, including line shapes and Ps-fractions as functions of temperature, density, and ionisation state: For low-energy ions, ^3He and α -particle reactions are the dominant contributors to β^+ -unstable isotopes during a flare, resulting in large abundances of ^{11}C , ^{13}N , ^{15}O , ^{17}F , and ^{18}F , depending on the initial $^3\text{He}/\alpha$ ratio and the ion spectral index. As soon as the energy per ion reaches beyond $\approx 300 \text{ MeV nucleon}^{-1}$, π^+ -production via proton-reactions is the only significant contribution to the e^+ -content. The slowing-down timescale from such e^+ s in the solar atmosphere is on the order of 20 s (Murphy et al, 2014) so that a significant amount of e^+ s annihilate directly in the atmosphere. Escape into the interplanetary medium may also be possible due to this timescale.

X-class solar flares are rare, but the only ones in which the 511 keV line has been detected, yet. Assuming that all flares produce e^+ s which annihilate either directly in the stellar atmosphere or escape the star and annihilate in their vicinity, Bisnovatyi-Kogan and Pozanenko (2017) estimated from a benchmark solar flare that 50–100% of the 511 keV line in the bulge may indeed be due to intermittently flaring stars. The model can easily be extended to include the Galactic disk. A relation between the 511 keV line flux and flare energy would refine this scenario as it is not clear how many e^+ s are really produced per flare and how many annihilate in situ. Such a scenario would immediately reduce the need for many different source types because the estimated and measured number for nucleosynthesis e^+ s would

now only need to explain a small fraction of the total flux. It would *also* reduce the need for far propagation (Sec. 3) because, as stated in Sec. 1.1, the stellar population already fits the data quite well. See Fig. 5 for an overview of the production rates of different models assumptions vs. the measured annihilation rate in the Milky Way.

A smoking gun evidence for a stellar flare scenario would be the detection of 511 keV lines from globular clusters that correlate with the number of stars in each cluster. Alternative scenarios in globular clusters are also possible, but they might show a different correlation, e.g. with the GeV flux from MSPs (Bartels et al, 2018).

3 Positron propagation

3.1 High-energy positrons

The propagation of e^+ s in the ISM is not well understood. From AMS-02, PAMELA, and other particle detectors around Earth, we know that at least high-energy e^+ s, with Lorentz-factors of $\gtrsim 1000$ reach Earth. Lower energy e^+ s are, similar to the case of other cosmic-ray species, heavily affected by the solar modulation potential. There appears to be an excess of cosmic-ray e^+ s above the expectations from secondary production of hadronic cosmic rays with the ISM that dominates the spectrum above ≈ 20 GeV (Aguilar et al, 2013, 2019). This component has been interpreted in terms of a nearby ($\lesssim 250$ pc) pulsar that manages to accelerate e^+ s to Lorentz factors of $\gtrsim 10^6$ (e.g., Di Mauro et al, 2014; Yin et al, 2013), or in terms of heavy (≈ 1.2 TeV) DM particles, co-annihilating into pairs (e.g., Kopp, 2013). While the first scenario may have been excluded by HAWC measurements (Abeysekara et al, 2017), the latter may be corroborated by ongoing measurements of AMS-02 within the next years. The fundamental problem in all of the scenarios is the assumption that cosmic-ray secondary production and e^+ -propagation in the Galaxy is understood.

Cowsik et al (2014) showed that the positron fraction $R_{e^+} = e^+/(e^+ + e^-)$, as measured by AMS-02, can be explained without additional sources. In their Nested Leaky-Box model, acceleration of cosmic rays happens in many sources across the Galaxy and e^+ -propagation follows the established works of Moskalenko and Strong

(1998), resulting in a source term with a power-law spectrum and spatial distribution according to the hydrogen density in the Galaxy. The propagation can then be described as spatial diffusion with radiative energy losses, and the leakage from the Galaxy, so that e^+ s may in fact escape on a characteristic time scale.

In summary, for highly relativistic e^+ s, even though we can measure directly the cosmic-ray spectrum at the position of the Solar System, it is not established, how e^+ s propagate in the ISM. An inaccurate assumption on the high-energy propagation led to conjectures of additional sources, but which may not be required at all if the premise is wrong.

3.2 Low-energy positrons

Now, in terms of low-energy e^+ s, either having Lorentz-factors of 1–3 in the case of nucleosynthesis e^+ s or a few 10s to 100s in the case of pulsars, the gross of secondary e^+ s from cosmic-ray interactions in the ISM (Murphy et al, 1987), pair-plasma ejections from XRBs, light DM particle annihilations, or Hawking radiation, we have no direct information on these particles. Therefore, we have to rely on theoretical assumptions as to how long and how far e^+ s propagate in the ISM, how many escape the Galaxy, how many annihilate in flight, and how many thermalise with the ISM.

Thermalisation:

The annihilation rates for cooled e^+ s ($\lesssim 10^7$ K; $\lesssim 1$ keV) in interstellar gas as a function of temperature are well understood (Guessoum et al, 2005), so that annihilation after thermalisation occurs inevitably after a characteristic timescale of about 1 Myr for ISM conditions of $T = 8000$ K and $n_{\text{H}} = 1 \text{ cm}^{-3}$. Panther et al (2018b) showed that including the much less abundant alkali metals in the ISM reduces this timescale to 0.1 Myr. Propagation after thermalisation is expected to follow the flow of the gas in which the e^+ s are thermalised, i.e. they will be advected rather than transported diffusively, and annihilate according to the conditions in the ISM. This is then either by charge exchange with hydrogen (only possible for kinetic energies > 6.8 eV, i.e. in gas with temperatures not much cooler than 5×10^4 K, but

also not hotter than 13.6 eV (10^5 K) as all hydrogen will be ionised) or by radiative recombination with free e^- s. The gas and e^- densities will determine the annihilation rate, given the e^+ density distribution and motion.

Collisional transport:

The processes between the injection of mildly relativistic e^+ s and the formation of Ps and final decay have been investigated in many studies (e.g., Prantzos, 2006; Jean et al, 2009; Martin et al, 2012; Alexis et al, 2014; Higdon et al, 2009; Rothschild, 2009; Siegert et al, 2021b). In collisional transport, e^+ s propagate almost ballistically and are guided by the large-scale magnetic field in the Galaxy. Through pitch-angle scatterings in a turbulent magnetic field, the generic stopping distance for e^+ s in typical ISM conditions is only reduced by 25% (Jean et al, 2009), resulting in an effective distance of $10 \left(\frac{n}{\text{cm}^{-3}}\right)^{-1}$ kpc. At MeV energies, e^+ energy losses are mainly due to ionisation and excitation of atoms, i.e. in general Coulomb interactions. Inverse Compton scattering, bremsstrahlung and synchrotron losses are only important for higher energies (\approx GeV) or when the gas density is small ($\lesssim 10^{-3} \text{ cm}^{-3}$), such as in the Galactic halo or in superbubbles. On the one hand, this length scale is larger than the typical phases of the warm ISM phase in which most e^+ s presumably annihilate as inferred from spectral analyses (Jean et al, 2006). On the other hand, Churazov et al (2011) showed that the 511 keV line profile is also consistent with annihilation in a cooling ISM, or within gas phases of temperatures around 100 K with only small ionisation fractions on the percent level. Both of these solutions appear realistic as the annihilation rate increases significantly when e^+ s approach denser regions, but the mixing from the hot ionised gas with HI regions or molecular clouds, for example at the edges of superbubbles, allows also warmer regions and a temperature and thus ionisation gradient (Krause et al, 2013). These ambiguous solutions may also imply that the assumed turbulence power spectrum has another shape, or that e^+ -propagation occurs through collisionless transport.

Collisionless transport:

In collisionless transport, e^+ s propagate according to pitch-angle scattering which may be described by an angular diffusion coefficient, and (re-)acceleration in a turbulent plasma which is governed by a momentum diffusion coefficient. The basis of this approach is that the gyroradii of $\gamma = 1-20$ e^+ s in multiphase ISM conditions ($B \approx 1-10 \mu\text{G}$), are on the order of 10^8-10^9 cm, much smaller than the ballistic length scale, so that the exact path of the e^+ can be averaged over the drift length scale. The cooling in collisionless transport then happens via particle interactions with magnetohydrodynamic (MHD) waves. In addition to e^+ -wave interactions, adiabatic losses, for example in Galactic ‘winds’ or expanding superbubbles, may be significant in this regime.

It is unknown how e^+ s propagate in the ISM: Different approaches that test the collisional or collisionless transport, either using Monte Carlo simulations (Alexis et al, 2014) or state-of-the-art cosmic-ray propagation codes (Martin et al, 2012), fall short in explaining the 511 keV morphology as measured with INTEGRAL/SPI. For example, Alexis et al (2014) expect that the spiral arm structure of the Milky Way would also be seen at 511 keV. Given the latest measurements, this is not detected.

3.2.1 Cosmic-ray transport equation

In general, the distribution of e^+ s as a function of time, position, and momentum, can be described as the solution of an appropriate Fokker-Planck-equation with *drift* (re-acceleration, convection, advection, energy losses), *diffusion* (coefficients due to transport mode and conditions), *source* (see Sec. 2), and *sink* (annihilation rates, cross sections, escape, leakage timescales) terms. Such a treatment requires realistic 3D-distributions of e^+ sources that are parametrised by their production rate and injection spectrum. As the β -decay spectrum is unique for different isotopes, the pair-plasma spectrum nearly thermal, pulsar e^+ s accelerated resulting in a power-law, and cosmic-ray secondary e^+ s peaking around 30 MeV, one cannot assume one generic spectrum for the injection in the Galaxy – and certainly no mono-energetic e^+ s. Furthermore, the gas (target) distributions cannot just be generic, smooth, models because the annihilation rates depend strongly on the varying

temperature, ionisation state, target density, and current e^+ -density. The energy losses also change as a function of the same parameters, so that an average gas component in such a model will never show the structure of where and at what temperature e^+ s really annihilate. Diffusion will also change as a function of Galactic component: For example could the Galactic wind from superbubble blowouts (Krause et al, 2021) be a region of either ballistic or advective transport up to 10 kpc into the halo. Above such a height, turbulence might set in again so that stronger diffusion could be expected. Similar arguments may be true for the bulge and disk as discussed in Higdon et al (2009). An important, albeit often neglected, term in the diffusion-convection equation is the destruction of e^+ s: It is typically assumed that e^+ s are removed from the scheme if their kinetic energy is below a threshold of, say, 100 eV (Martin et al, 2012). This assumption may be flawed since the cooling down time scale for MeV e^+ s is on the order of Myr whereas the annihilation timescale after thermalisation might be similar. The timescales depend on the exact conditions of the ISM at the time, but the cooling down time is generally larger than the annihilation time after thermalisation (Guessoum et al, 2005; Jean et al, 2009). Nevertheless, in a time of 0.1–1 Myr, interstellar gas, especially in low-density regions, may be propagating 10–100 pc and therefore significantly changing the annihilation morphology.

3.2.2 Annihilation in flight

Martin et al (2012) also included the process of e^+ -annihilation ‘in flight’, i.e. the direct annihilation of e^+ s with e^- s without forming Ps first, that also removes e^+ s from the scheme. This process is only governed by the annihilation cross section as a function of energy, given the densities of the interacting particles. There appears to be a consensus that annihilation in flight is negligible for MeV e^+ s because of two reasons: 1) The probability that this process is happening at higher energies is very low, and 2) Beacom and Yüksel (2006) and Sizun et al (2006) claim that the annihilation in flight of e^+ s must not happen at energies above several MeV due to spectral constraints. I will argue here that both these reasons should be considered only on the premise of a steady state between production and annihilation *inside* the Galaxy, and that

the model comparison to the available data was inadequately performed.

About 1): If it is assumed that e^+ s are injected mono-energetically with initial energy E_i (which is never the case, except for maybe DM), in an ISM of number density n_H and temperature $\lesssim 10^5$ K, with Lorentz-factors $\gamma \lesssim 100$, the dominant cooling process is ionisation and excitation of ambient gas. If only this process is considered, then the survival probability, P , i.e. not annihilating in flight, is always greater than 80 %, rising with decreasing kinetic energy. The in-flight annihilation flux, F_{IA} , is calculated as (Beacom and Yüksel, 2006)

$$F_{IA} = F_{511} \frac{1}{1 - \frac{3}{4} f_{Ps}} \frac{1 - P}{P} := r_{IA} F_{511}, \quad (13)$$

where f_{Ps} is the (measured) Ps fraction from the ratio of the 511 keV line and the ortho-Ps continuum, $0 \leq r_{32} \leq 4.5$ (Ore and Powell, 1949). For a canonical value of f_{Ps} close to 1 as suggested by measurements, the total in-flight annihilation flux is at most the 511 keV line flux, but distributed over a wide continuum (see Fig. 6). The smaller the injection energy, the smaller the total in-flight annihilation flux, and the less pronounced is the high-energy bump corresponding to the injection energy (minus $m_e/2$). However, this is not the only energy loss possible in the ISM: If the kinetic energy of the e^+ s is smaller than the plasma temperature of, say $k_B T \lesssim 10$ keV, temperature-dependent losses set in, and can be orders of magnitude larger than the ionisation losses. Clearly, the ionisation fraction would also be close to one, replacing ionisation losses with Coulomb losses. Such high temperatures may be found in hot gas with lower densities such as in superbubbles or the Galactic halo, lowering the survival probability and the resulting normalisation of the in-flight annihilation flux.

In addition to the potentially increased flux for annihilation in flight, the premise of ‘all e^+ s are annihilating’ may not hold in the light of INTEGRAL/SPI observations: As stated above, coded aperture masks can only hardly observe isotropic emission, such as would be plausible for a halo component. Hydrodynamics simulations suggest that radioactive isotopes, and therefore the starting points of e^+ -propagation, can reach very high distances above the Galactic plane (Krause et al, 2021). If e^+ s are emitted at heights of 2 kpc or

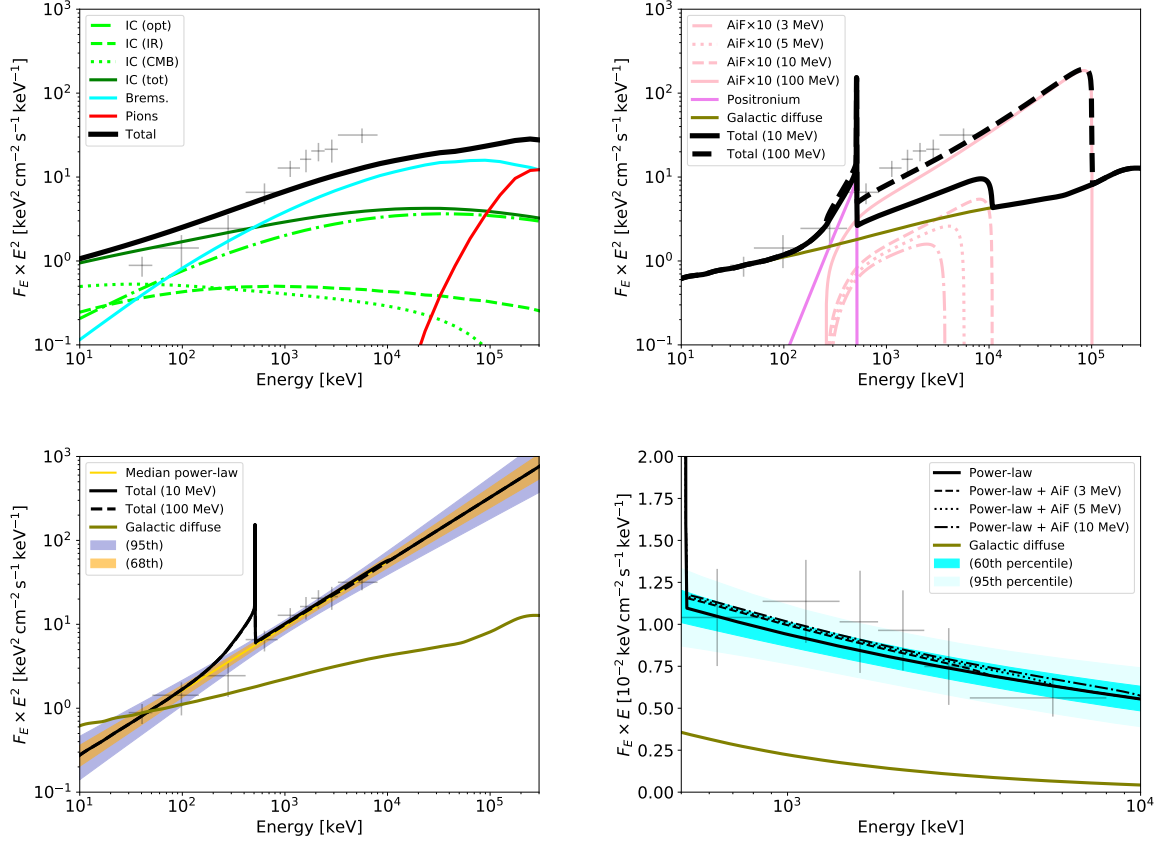


Fig. 6 Diffuse MeV continuum spectrum possibilities of the Milky Way in the range $l \leq 47.5^\circ$, $b \leq 47.5^\circ$. The gray data points indicate the measured Milky Way spectrum between 0.03 and 8 MeV with INTEGRAL/SPI (Siegert et al, 2022a; Berteaud et al, 2022), excluding the γ -ray lines at 511 keV and 1809 keV, as well as the ortho-Ps continuum. **Top left:** Generic GALPROP model components can roughly explain the entire spectrum with Inverse Compton (IC) emission from the CMB, infrared (IR) light, and optical (opt, scaled up by a factor of 2, suggested by Bouchet et al (2011), for example) light, and a bremsstrahlung component (scaled up by a factor of 3 to roughly match the data). **Top right:** The Galactic diffuse baseline model (no scalings) allows for additional components, such as e^+ -annihilation in flight. A ten times stronger than measured flux of e^+ -annihilation allows annihilation in flight up to injection energies above 100 MeV. **Bottom left:** A power-law description (shaded bands for 1 and 2σ uncertainties) would explain the data completely, but would disagree with a Galactic diffuse baseline model. **Bottom right:** Zoom in to the fit from the bottom left plot, in the style of Beacom and Yüksel (2006), but extended to the entire region of interest. Assuming the fitted power-law explains the entire emission, within uncertainties, the annihilation in flight injection energy is automatically constrained to below 10 MeV. Work in progress / preliminary results by Siegert et al. (2023, in prep.).

higher, they may propagate freely in the halo medium and eventually annihilate on the border to the IGM. Unless the e^+ s are guided back to Galaxy (e.g., Prantzos, 2006), they have no preferential target to annihilate with. This could then result in an isotropic component but which would be invisible for current γ -ray telescopes. As suggested in Sec. 2, the production rate in the Milky Way might be a factor of five or more larger than what is *seen* to annihilate. If such an additional component exists, the e^+ -annihilation in flight

spectrum might in fact be larger by about this factor (integrated over the whole sky, but with a possibly different morphology).

About 2): It has been suggested that the injection energy of e^+ s into the ISM must not be larger than 3–7 MeV, based on model comparisons to already-extracted flux data points without taking into account the energy dispersion of the used γ -ray instruments (e.g., Beacom and Yüksel, 2006; Sizun et al, 2006). This claim originates from the

fact that it is assumed that the diffuse γ -ray continuum emission in the Milky Way is understood, and only taking into account a region with a radius of 5° around the Galactic centre. Similar to the case of high-energy cosmic-ray e^+ s (see Sec. 3.1), the former is not the case.

In particular, it was assumed that the MeV spectrum can be described by a power-law, which is certainly the case, given the uncertainties of the data points (see Fig. 6). However, searching for an additional component *above* this power-law without allowing to change the power-law parameters in a spectral fit, will never find an additional component, because the power-law *already* describes the data well. This means an annihilation in-flight spectrum has to be as small as to not ‘overshoot’ the power-law model, which results in an inevitable upper bound on the injection energy of 3–7 MeV, because the total flux is bound to the 511 keV line flux.

Now, if an astrophysical model is assumed for the diffuse γ -ray continuum, for example calculated with GALPROP (Strong et al, 2007), the model is parametrised with the cosmic-ray e^- spectrum, i.e. its spectral shape and amplitude, with the interstellar radiation field, with the particle density (for bremsstrahlung and pion-production), and with the magnetic field, among other parameters. Such a parametrisation allows for a much more flexible model, and, given the uncertainties of the measurements in the MeV range as well as from direct cosmic-ray measurements and high-energy γ -rays, results in a less-determined spectrum than by just fitting a power-law (see Fig. 6). The reason why the e^+ injection energy appears to be bound to several MeV is because a model is assumed that already fully explains the data.

In Fig. 6, I show four cases that are compatible with the MeV data and still allowed by other constraints from cosmic rays and GeV γ -rays. It is clear that from the MeV γ -ray spectrum alone, the annihilation in flight spectrum and therefore injection energies, cannot be determined – at least with current instrumentation. A precise statement requires a broader spectral range, must also take into account the measured cosmic-ray e^- spectrum at GeV energies, and must allow for different cosmic-ray populations in the Galaxy.

4 Future avenues

The Positron Puzzle appears to require a smoking-gun-evidence measurement to proceed. But solving the puzzle does not only rely on better measurements with future instrument – of course the latter will tremendously help –, it also relies on understanding the MeV sky itself better as well as more solid data analyses.

4.1 Foreground emission

While the 511 keV line is the strongest astrophysical γ -ray line known, the will to take ‘pictures’ of the MeV sky unavoidably results in ambiguities, image reconstruction artefacts, and finally doubt about the results. But many of the low-significance features in MeV images might in fact not be artefacts but due to a time variable foreground emission. As described in Sec. 2.2, the cosmic-ray bombardment of small Solar System bodies leads to nuclear excitation and pion production, followed by de-excitation via γ -ray emission and e^+ -annihilation on top of a bremsstrahlung spectrum. It is known from γ -ray measurements of the asteroid 433 Eros (Peplowski, 2016), that there is indeed a 511 keV line, plus de-excitation lines that inform about the asteroid’s composition. From the entire population of asteroids in the main belt between Mars and Jupiter (torus at 2.0–3.5 AU), the Kuiper belt beyond Neptune (torus at 30–50 AU), the Jovian trojans (accumulation at Lagrange points of the Jupiter-Sun-system; orbital time 11 yr), the plausible Neptunian trojans (orbital time 165 yr), and the suspected but not proven Oort-cloud (spherical accumulation between 10^3 – 10^5 AU) would all contribute to a time variable foreground emission, predominantly in the ecliptic (see also Moskalenko et al, 2008, for estimates). The Oort-cloud, if real, would even lead to an isotropic 511 keV, and in general broadband MeV, emission. For coded aperture masks, this emission would be invisible, but would be detected by Compton telescopes, such as the Compton Spectrometer and Imager (COSI, Tom-sick et al, 2019, planned for launch in 2027), if the flux is large enough. The ecliptic has an intriguing overlap with the Galaxy, almost exactly at the Galactic bulge, so that the bulge emission at 511 keV with a flux of 10^{-3} ph cm $^{-2}$ s $^{-1}$ could actually be expected to change as a function of

planetary time scales by 1–5%. Such a measurement is on the verge of possibilities with current instrumentation. Since the ecliptic is rarely observed with INTEGRAL/SPI, the possibility to detect the foreground emission directly requires a time variable diffuse emission model. If emission from apparently moving sources is analysed time independent, their resulting picture, or map, may include high-flux regions which can hardly be explained by astrophysical sources outside the Solar System.

The 511 keV line sensitivity we would need to identify the time-averaged components we probably already have with INTEGRAL/SPI, about $8 \times 10^{-5} \text{ ph cm}^{-2} \text{ s}^{-1}$ (3σ point source sensitivity for 1 Ms). But the current exposure of SPI, being mostly concentrated along the Galactic plane and bulge, makes it difficult to identify any high-latitude component. Since the individual components would be large on the sky, possibly with several tens of degrees in diameter, the line sensitivity to disentangle these foreground components should be below $10^{-5} \text{ ph cm}^{-2} \text{ s}^{-1}$. The future COSI-SMEX mission (Tomsick et al, 2019) will shed light on the Solar System foreground.

4.2 Isotropic Emission

In addition to the Oort cloud, there may be even more isotropic components, especially for the 511 keV line. From the Nested Leaky-Box-Model of Cowsik et al (2014), it is clear that a large portion of e^+ s may leave the Galaxy. But also in the Galactic halo and the IGM, e^+ s would eventually find their e^- s to annihilate with. Depending on the temperature where e^+ s recombine with e^- s, the 511 keV line would be broadened accordingly. Given the direct measurements, and accounting for all uncertainties, even within 1σ , more than five times the e^+ s *seen to annihilate* could be produced in the Milky Way. Within 2σ , up to a factor of ten is possible. Only with a Compton telescope or vastly improved coded-mask apertures, or in general MeV telescopes, could such an isotropic component be detected from the Milky Way.

A similar isotropic emission component at 511 keV might be expected from DM, as the line-of-sight integration into all directions always leads to an offset, which would result in an isotropic part. From the CGB, such a component would then also include a red-shift dependence, so that

both, a strong 511 keV line, and a continuum-like component due to integration across red-shifts would be expected (Iguaz et al, 2021).

Finally, also the pair-absorption of very- and ultra-high-energy photons will create e^-e^+ -pairs in the Galaxy and the IGM which will eventually annihilate and plausibly produce an isotropic 511 keV line. The mean free path of PeV photons, for example, is less than 10 kpc so that any ‘pevatron’ inside the Galaxy will also create e^+ s through pair production with the CMB and the interstellar radiation field. For extragalactic sources, this also applies, and the shear number of extragalactic $>\text{TeV}$ sources will lead to the inevitable pair production in the IGM.

The possibility of an isotropic 511 keV line is an going research topic and there are hardly any flux expectations or predictions. As mentioned above, coded aperture masks can hardly identify isotropic emission unless specific satellite orbit manoeuvres are performed. INTEGRAL Earth occultation observations allowed us to measure the cosmic X-ray background up to $\sim 200 \text{ keV}$, but did not consider the 511 keV line (e.g. Churazov et al, 2007; Türler et al, 2010). A current all-sky sensitivity of SPI of $10^{-2} \text{ ph cm}^{-2} \text{ s}^{-1}$ is estimated from the previous results. A ten-fold sensitivity improvement in the 511 keV line might already show if there are e^+ s annihilating in the halo which current instruments are blind for.

4.3 Imaging might not be enough

With new MeV telescopes, i.e. improved angular resolution and better sensitivity, new images of the 511 keV sky will be created. But even with the identification of 511 keV point sources, there may be open questions, as to why the morphology is what it is. The comparison of tracer maps, and ranking them according to relative likelihoods gives an idea of what the sources or sinks are, but the physics cannot be probed on this basis.

Pleintinger et al (2019) tried to disentangle the overall morphology of the ^{26}Al line at 1809 keV by slicing the data into longitude-bins and measuring the scale height by a maximum likelihood fit. The regions were chosen independent from each other, so that a statistic about scale heights could be generated. From Hydrodynamics simulations, for example, or population synthesis calculations, a similar statistic can then be calculated which

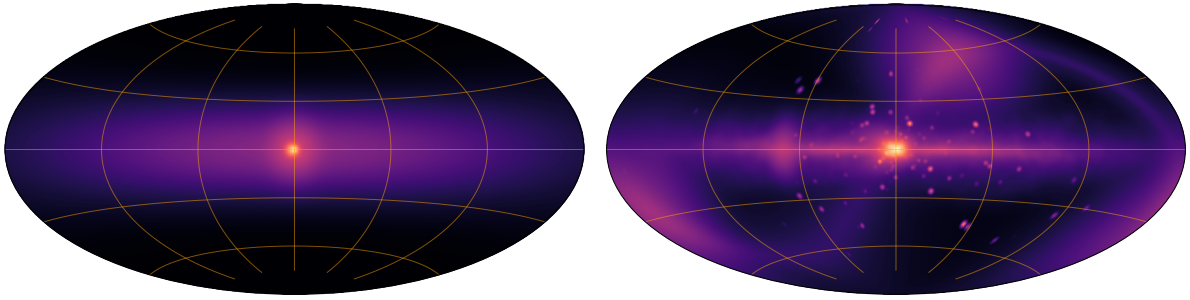


Fig. 7 Positron annihilation in the Galaxy. *Left:* Four-component model from Siegert et al (2016b) that describes the INTEGRAL/SPI data completely. *Right:* Astrophysically motivated model of annihilation emission, including old stars (boxy bulge, nuclear stellar cluster and disk, infrared disk; intermittently flaring stars), globular clusters (point-like), spiral arm structure (HI annihilation regions), dominant massive star regions (e.g. Cygnus OB2, Orion), plus foreground emission (main belt asteroids and Jovian trojans) along the ecliptic. Dark matter halo and isotropic components are not shown. The sensitivity (lower flux limit) of the right image is about a factor of 20 better than in the left image.

includes all the astrophysical input. From this treatment it was found that indeed, chimney-like structures could exist in the Galaxy, which was not possible before.

A more advanced approach would be a decomposition similar to the CMB power spectrum. If the raw data, or in a weaker version the reconstructed images, can be analysed through spherical harmonics, a meaningful multipole series expansion up to $l \approx 100$ would be possible with future telescopes. In this way, the physical interpretation does not rely dramatically on the background model, and inferences from costly hydrodynamics simulations are made possible. Especially in the case of the 511 keV emission with its many source distributions, the full (unknown) propagation, and final annihilation sites, will benefit from structured, high-resolution, simulations to understand the full impact of the puzzle.

Structural comparisons will be better the better the sensitivity of the instrument and the more homogeneous the exposure. Size and angular scales can be more solidly compared if the sensitivity is improved by another decade with respect to INTEGRAL/SPI, for example. The COSI-SMEX mission will have a 511 keV line point source sensitivity of less than 10^{-5} ph cm⁻² s⁻¹ for each position in the sky after its two-year nominal mission, thanks to its large field of view of 1π sr (Tomsick et al, 2019).

4.4 What gives?

With new measurements from a new telescope, further analyses towards understanding the MeV

foreground, and data analysis tools that focus on the astrophysical parameters, the Positron Puzzle may solve more than just the origin of e⁺s in galaxies. With current instrumentation, it is already now possible to develop astrophysical models that are bound by the total emission in the Galaxy. The 511 keV line, and associated also the ortho-Ps continuum as well as the in-flight annihilation component, can be used to study other unsolved problems in astrophysics. I will outline two examples here that have, at first glance, nothing in common, but are indeed connected through e⁺-annihilation.

Dark matter:

As described above, DM in the form of beyond-standard-model particles or PBHs will eventually lead to non- or highly-relativistic e⁺s, or a mixture in between. These e⁻s and e⁺s will be responsible for additional spectral components from GHz to GeV. As the PBHs evaporate or DM particles co-annihilate, the secondary particles will decay and result in a prompt emission spectrum around the scale of the PBH or DM mass, typically peaking at about 10% of the particles' masses. The secondary high-energy e⁻s and e⁺s created propagate diffusively and experience losses from IC scattering off of CMB and infrared/optical photons (e.g., Saxena et al, 2011; Cirelli and Panci, 2009). This would create a characteristic IC bump that should be consistent throughout all astrophysical observation possibilities (Milky Way, dwarf galaxies, isotropic with redshift integration). For GeV pairs, this would result in peaks in the MeV

range (see Fig. 6). In addition will the pairs experience synchrotron losses, so that a characteristic synchrotron spectrum would be visible, also with a peak that depends on the pairs' energies and hence the initial DM particle mass. When the pairs are then cooled and the IC, synchrotron and bremsstrahlung losses are sub-dominant, Coulomb losses set in, and e^- s and e^+ s require on the order of 0.1–10 Myr to cool down to thermal temperatures (see Sec. 3.2). During this entire time, the e^+ s may also annihilate in flight, leading to another characteristic feature that depends on the initial e^+ spectrum. Then, after thermalisation, e^+ s eventually annihilate via the formation of Ps, showing the strong 511 keV line and the ortho-Ps component.

Building a full model of the secondary and tertiary particles from DM annihilation (or PBH evaporation) in the Milky Way, and adequately comparing this to the available data from radio to γ -rays is difficult as the astrophysical foreground has to be understood. But especially the IC MeV continuum and 511 keV line are orthogonal to most other wavelengths (see Fig. 1) in which a 'prompt' DM annihilation may be visible. This makes them an invaluable messenger in the indirect search for DM. The cosmic-ray e^+ s and e^- s, for example measured with AMS-02, should also be used to constrain the DM searches *in addition* to photon observations – not independently.

Solar coronal heating problem:

Assuming instead that the 511 keV emission that is coincident with the positions of stars (i.e. a considerable fraction, see Fig. 3) comes from stellar flares, one can build a model to determine the lower and upper cut-off energy of the flare-frequency-energy distribution. Determining the lower cut-off energy from the entire population of stars may inform the solar coronal heating problem as it is believed that micro- and nano-flares are responsible for the high temperatures of the Sun's corona. Instead of observing a single star in 511 keV, which is only possible for the Sun, the Galactic 511 keV emission provides a means to observe *all* stars at the same time. For such an endeavour, one needs to build a hierarchical model that eventually predicts the total flux at 511 keV (and ortho-Ps). Again, for the entire Milky Way, such a model will be difficult, but hotspots, such

as expected from globular clusters, would result in characteristic ratios among the 157 globular clusters of the Milky Way (Harris, 2010). Such a ratio will be very rigid so that different models, which may also be tested in globular clusters (Bartels et al, 2018), could easily be distinguished.

In particular, for each of the $N = j$ globular clusters of the Milky Way, an initial mass function (IMF) with shape Γ_j and total number of stars N_{j*} determines the masses M_* of stars in each object. Each star with mass M_* has its own flare-frequency-energy distribution that determines the average number of e^+ s in each flare. The flare distribution depends on three parameters, the low-energy cut-off, E_{lo} , high-energy cut-off E_{hi} , and a steepness parameter α , where E_{lo} and E_{hi} could also depend on the stellar mass. The star's mass also determines the density profile, n_* , of the stellar atmosphere, from which finally the number of annihilation photons (flux) can be calculated. Given the distances to all globular clusters in the Milky Way, a flux pattern of 511 keV point sources would be result (see Fig. 7, right). The only fitted parameters of such a model would be E_{lo} and E_{hi} since other parameters would be determined from independent measurements. These cut-offs serve as normalisation parameters for the final 511 keV flux because if E_{lo} is too small or E_{hi} too large, too many stars would flare too frequently, so that the globular clusters would appear brighter than what is actually measured.

Based on a correlation with the GeV flux (Bartels et al, 2018), one can estimate to an order of magnitude how bright several objects would be in the 511 keV line. There could be 19 globular cluster with a flux of 10^{-6} ph cm⁻² s⁻¹ or more, with Omega Centauri, 47 Tucanae, Terzan 5, and NGC 6397 as potentially the brightest ones with fluxes of $(1-2) \times 10^{-5}$ ph cm⁻² s⁻¹. COSI would easily detect these objects within its two year mission (Tomsick et al, 2019). The total 511 keV flux of all globular cluster combined would be around 2×10^{-4} ph cm⁻² s⁻¹. Only a few objects would be seen individually, but since they follow a certain hierarchy given their GeV fluxes, they can be treated as one population and discovered as one entity.

For a stellar flare scenario (Bisnovatyi-Kogan and Pozanenko, 2017), i.e. roughly scaling with stellar mass, the expected fluxes would be mostly below 10^{-6} ph cm⁻² s⁻¹ for individual objects.

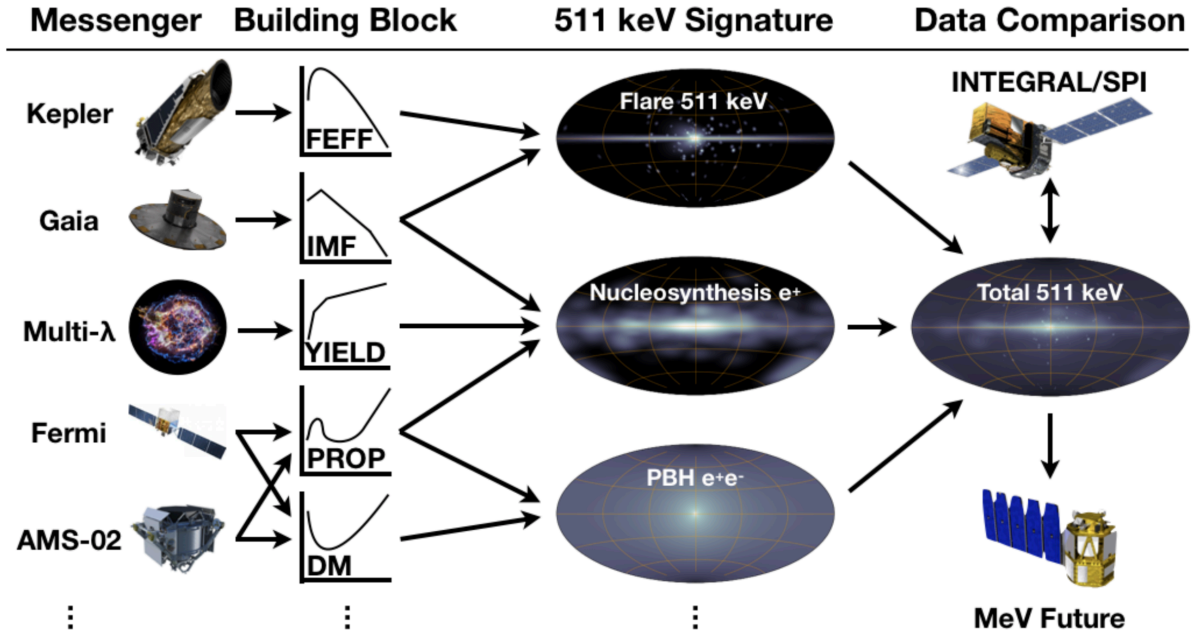


Fig. 8 Model and observational components required to solve the Positron Puzzle. From left to right, the messengers (multi-wavelength and cosmic-ray measurements) inform the building blocks of an intertwined (hierarchical) model, that provides the flare-energy-frequency function (FEFF), the IMF, the nucleosynthetic yields (of β^+ -decayers), the propagation parameters, and DM limits, among others. The building blocks are used to create e^+ -source-specific images at 511 keV and all other components (ortho-Ps, annihilation in flight, IC, etc.), which can then be fitted to the raw data of current (INTEGRAL/SPI) and future (e.g., COSI) instruments sensitive to e^+ -annihilation.

Again Omega Centauri and 47 Tucanae would be the brightest, but not individually detectable, even with COSI. The total flux of all 157 objects would be on the edge of the detection limit for future instruments in the case of a 511 keV line purely from stellar flares.

5 Putting it all together

It is clear that both exemplary models from above, DM and stellar flares, may in fact contribute to the entire Galactic signal. Extrapolating the models from individual objects to the entire Milky Way signal will turn out to be more complex as they might be interdependent – but are bound by the morphology and total flux measured. Such models, if e^+ -transport is properly taken into account, can actually be *fitted* to data instead of just building the advanced models. The resulting 3D emissivities need to be line-of-sight integrated which leads to 2D-images, parametrised by only a few parameters, similar to heuristic models but with physical meaning. The final all-sky images (i.e. the Milky Way, plus *all* other contributions from

dwarf galaxies, globular clusters, nearby sources, isotropic emission), and spectral differences (not just the 511 keV line but annihilation in hot gas, Ps fraction, annihilation in flight, IC components, etc.) can be directly compared to raw data of instruments.

In order to build a full understanding of the Positron Puzzle, it cannot be solved by arguing about individual sources – they must all be described together. This means that for each e^+ -source population, a realistic e^+ -production mechanism, escape, and injection to the ISM needs to be built. But all these source populations and injected e^+ s are required to experience the same propagation mechanism through which the final annihilation image is tied together. If the e^+ s do not escape, a fraction of the Galactic 511 keV emission will come from in-situ annihilation, for example from stellar flares and SN remnants.

The two important messages to understand here are: 1) Occam’s razor must not be misinterpreted in the case of finding *the* source responsible for annihilating e^+ s in the Milky Way. It is clear from a multitude of observational evidence that

there must be more than one source that contributes to the entire measured signal. 2) Only by considering more data than just the 511 keV line will lead to reasonable progress in solving the Positron Puzzle (Fig. 8). In turn, by having this unique astrophysical messenger, we will gain insights to other unsolved astrophysical problems.

Supplementary information. Not applicable

Acknowledgments. I thank Martin G. H. Krause, Karl Mannheim, Roland Diehl, Jochen Greiner, John Tomsick, and Steve Boggs for support throughout the years and for fruitful discussions.

Declarations

Not applicable.

Editorial Policies for:

Springer journals and proceedings:
<https://www.springer.com/gp/editorial-policies>

Nature Portfolio journals: <https://www.nature.com/nature-research/editorial-policies>

Scientific Reports: <https://www.nature.com/srep/journal-policies/editorial-policies>

BMC journals: <https://www.biomedcentral.com/getpublished/editorial-policies>

References

- Abeyssekara AU, Albert A, Alfaro R, et al (2017) Extended gamma-ray sources around pulsars constrain the origin of the positron flux at earth. *Science* 358(6365):911–914. <https://doi.org/10.1126/science.aan4880>
- Ackermann M, Ajello M, Allafort A, et al (2013) Detection of the Characteristic Pion-Decay Signature in Supernova Remnants. *Science* 339:807–811. <https://doi.org/10.1126/science.1231160>, URL <http://arxiv.org/abs/1302.3307>
- Aguilar M, Alberti G, Alpat B, et al (2013) First Result from the Alpha Magnetic Spectrometer on the International Space Station: Precision Measurement of the Positron Fraction in Primary Cosmic Rays of 0.5–350 GeV. *Physical Review Letters* 110(14):141,102. <https://doi.org/10.1103/PhysRevLett.110.141102>
- Aguilar M, Ali Cavasonza L, Ambrosi G, et al (2019) Towards Understanding the Origin of Cosmic-Ray Positrons. *Physical Review Letters* 122(4):67. <https://doi.org/10.1103/PhysRevLett.122.041102>, URL <https://link.aps.org/doi/10.1103/PhysRevLett.122.041102>
- Aharonian FA, Atoyan AM, Voelk HJ (1995) High energy electrons and positrons in cosmic rays as an indicator of the existence of a nearby cosmic tevatron 294:L41–L44
- Albernhoe F, Le Borgne JF, Vedrenne G, et al (1981) Detection of the positron annihilation gamma ray line from the Galactic Center region. *Astronomy & Astrophysics* 94:214–218. URL <http://adsabs.harvard.edu/abs/1981A&A....94..214A>
- Alexis A, Jean P, Martin P, et al (2014) Monte Carlo modelling of the propagation and annihilation of nucleosynthesis positrons in the Galaxy. *Astronomy & Astrophysics* 564:A108. <https://doi.org/10.1051/0004-6361/201322393>, URL http://adsabs.harvard.edu/cgi-bin/nph-data_query?bibcode=2014A%26A...564A.108A&link_type=EJOURNAL
- Arnett WD (1982) Type I supernovae. I - Analytic solutions for the early part of the light curve 253:785–797
- Baganoff FK, Maeda Y, Morris M, et al (2003) Chandra X-Ray Spectroscopic Imaging of Sagittarius A* and the Central Parsec of the Galaxy 591:891–915. <https://doi.org/10.1086/375145>
- Bandyopadhyay RM, Silk J, Taylor JE, et al (2009) On the origin of the 511-keV emission in the Galactic Centre. *arXiv.org* 392:1115–1123. <https://doi.org/10.1111/j.1365-2966.2008.14113.x>, URL <http://arxiv.org/abs/0810.3674>
- Bartels R, Calore F, Storm E, et al (2018) Galactic binaries can explain the Fermi Galactic centre excess and 511 keV emission. *Monthly Notices of the Royal Astronomical Society* 480(3):3826–3841. <https://doi.org/10.1093/mnras/sty2135>,

- URL http://adsabs.harvard.edu/cgi-bin/nph-data_query?bibcode=2018MNRAS.480.3826B&link_type=EJOURNAL
- Beacom JF, Yüksel H (2006) Stringent Constraint on Galactic Positron Production. *Physical Review Letters* 97(7):071,102—. <https://doi.org/10.1103/PhysRevLett.97.071102>, URL <http://dx.doi.org/10.1103/PhysRevLett.97.071102>
- Beloborodov AM (1999) Electron-positron outflows from gamma-ray emitting accretion discs 305:181–189. <https://doi.org/10.1046/j.1365-8711.1999.02384.x>
- Bennett CL, Larson D, Weiland JL, et al (2013) Nine-year Wilkinson Microwave Anisotropy Probe (WMAP) Observations: Final Maps and Results. *arXivorg* 208:20. <https://doi.org/10.1088/0067-0049/208/2/20>, URL <http://arxiv.org/abs/1212.5225>
- Berteaud J, Calore F, Iguaz J, et al (2022) Strong constraints on primordial black hole dark matter from 16 years of INTEGRAL/SPI observations. *arXivorg* p *arXiv:2202.07483*. URL <http://adsabs.harvard.edu/abs/2022arXiv220207483B>, <https://arxiv.org/abs/2202.07483>
- Bisnovatyi-Kogan GS, Pozanenko AS (2017) Can Flare Stars Explain the Annihilation Line from the Galactic Bulge? *Astrophysics* 60(2):223–227. <https://doi.org/10.1007/s10511-017-9477-6>, URL <https://link.springer.com/article/10.1007/s10511-017-9477-6>
- Bjorklund R, Crandall WE, Moyer BJ, et al (1950) High energy photons from proton-nucleon collisions. *Physical Review* 77(2):213–218. <https://doi.org/10.1103/physrev.77.213>
- Boehm C, Hooper D, Silk J, et al (2004) MeV Dark Matter: Has It Been Detected? *Physical Review Letters* 92(10):101,301. <https://doi.org/10.1103/PhysRevLett.92.101301>, URL <https://journals.aps.org/prl/abstract/10.1103/PhysRevLett.92.101301>
- Bouchet L, Mandrou P, Roques JP, et al (1991) Sigma discovery of variable e(+)-e(-) annihilation radiation from the near Galactic center variable compact source 1E 1740.7 - 2942. *Astrophysical Journal* 383:L45–L48. <https://doi.org/10.1086/186237>, URL <http://adsabs.harvard.edu/doi/10.1086/186237>
- Bouchet L, Roques JP, Jourdain E (2010) On the Morphology of the Electron-Positron Annihilation Emission as Seen by Spi/integral. *The Astrophysical Journal* 720(2):1772–1780. <https://doi.org/10.1088/0004-637X/720/2/1772>, URL http://adsabs.harvard.edu/cgi-bin/nph-data_query?bibcode=2010ApJ...720.1772B&link_type=EJOURNAL
- Bouchet L, Strong AW, Porter TA, et al (2011) Diffuse Emission Measurement with the SPectrometer on INTEGRAL as an Indirect Probe of Cosmic-Ray Electrons and Positrons. *The Astrophysical Journal* 739(1):29. <https://doi.org/10.1088/0004-637X/739/1/29>, URL http://adsabs.harvard.edu/cgi-bin/nph-data_query?bibcode=2011ApJ...739...29B&link_type=EJOURNAL
- Caroli E, Stephen JB, Di Cocco G, et al (1987) Coded aperture imaging in X- and gamma-ray astronomy. *Space Science Reviews* 45(3):349–403. <https://doi.org/10.1007/BF00171998>, URL <https://link.springer.com/article/10.1007/BF00171998>
- Castor J, McCray R, Weaver R (1975) Interstellar bubbles 200:L107–L110. <https://doi.org/10.1086/181908>
- Cheng KS, Ho C, Ruderman M (1986) Energetic radiation from rapidly spinning pulsars. I - Outer magnetosphere gaps. II - VELA and Crab 300:500–539. <https://doi.org/10.1086/163829>
- Cheng KS, Chernyshov DO, Dogiel VA (2007) Diffuse gamma-ray emission from the Galactic center - a multiple energy injection model. *arXivorg* 473:351–356. <https://doi.org/10.1051/0004-6361:20077538>, URL <http://arxiv.org/abs/0706.4351>
- Churazov E, Sunyaev R, Sazonov S, et al (2005) Positron annihilation spectrum from the

- Galactic Centre region observed by SPI/INTEGRAL. *Monthly Notices of the Royal Astronomical Society* 357(4):1377–1386. <https://doi.org/10.1111/j.1365-2966.2005.08757.x>, URL http://adsabs.harvard.edu/cgi-bin/nph-data_query?bibcode=2005MNRAS.357.1377C&link_type=EJOURNAL
- Churazov E, Sunyaev R, Revnivtsev M, et al (2007) INTEGRAL observations of the cosmic X-ray background in the 5-100 keV range via occultation by the Earth. *Astronomy & Astrophysics* 467(2):529–540. <https://doi.org/10.1051/0004-6361:20066230>, URL http://adsabs.harvard.edu/cgi-bin/nph-data_query?bibcode=2007A%26A...467.529C&link_type=EJOURNAL
- Churazov E, Sazonov S, Tsygankov S, et al (2011) Positron annihilation spectrum from the Galactic Centre region observed by SPI/INTEGRAL revisited: annihilation in a cooling ISM? *Monthly Notices of the Royal Astronomical Society* 411(3):1727–1743. <https://doi.org/10.1111/j.1365-2966.2010.17804.x>, URL http://adsabs.harvard.edu/cgi-bin/nph-data_query?bibcode=2011MNRAS.411.1727C&link_type=EJOURNAL
- Churazov E, Sunyaev R, Isern J, et al (2014) Cobalt-56 γ -ray emission lines from the type Ia supernova 2014J. *Nature* 512(7):406–408. <https://doi.org/10.1038/nature13672>, URL http://adsabs.harvard.edu/cgi-bin/nph-data_query?bibcode=2014Natur.512.406C&link_type=EJOURNAL
- Cirelli M, Panci P (2009) Inverse Compton constraints on the dark matter e+e-excesses. *NuclPhysB*821:399-416,2009 <https://doi.org/10.1016/j.nuclphysb.2009.06.034>, <https://arxiv.org/abs/0904.3830> [astro-ph.CO]
- Cowsik R, Burch B, Madziwa-Nussinov T (2014) THE ORIGIN OF THE SPECTRAL INTENSITIES OF COSMIC-RAY POSITRONS. *The Astrophysical Journal* 786(2):124. <https://doi.org/10.1088/0004-637x/786/2/124>
- Crocker RM, Ruiter AJ, Seitzzahl IR, et al (2017) Diffuse Galactic antimatter from faint thermonuclear supernovae in old stellar populations. *Nature Astronomy* 1:0135. <https://doi.org/10.1038/s41550-017-0135>, URL <http://arxiv.org/abs/1607.03495>
- Dame TM, Hartmann D, Thaddeus P (2001) The Milky Way in Molecular Clouds: A New Complete CO Survey. *The Astrophysical Journal* 547(2):792–813. <https://doi.org/10.1086/318388>, URL http://adsabs.harvard.edu/cgi-bin/nph-data_query?bibcode=2001ApJ...547.792D&link_type=EJOURNAL
- Di Mauro M, Donato F, Fornengo N, et al (2014) Interpretation of AMS-02 electrons and positrons data. *arXiv* 4:006. <https://doi.org/10.1088/1475-7516/2014/04/006>, URL <http://arxiv.org/abs/1402.0321>
- Dickey JM, Lockman FJ (1990) H I in the Galaxy. IN: *Annual review of astronomy and astrophysics Vol 28 (A91-28201 10-90)* Palo Alto 28(1):215–261. <https://doi.org/10.1146/annurev.aa.28.090190.001243>, URL <http://www.annualreviews.org/doi/10.1146/annurev.aa.28.090190.001243>
- Diehl R, Halloin H, Kretschmer K, et al (2006) Radioactive ²⁶Al from massive stars in the Galaxy. *Nature* 439(7072):45–47. <https://doi.org/10.1038/nature04364>, URL <https://www.nature.com/articles/nature04364>
- Diehl R, Siebert T, Hillebrandt W, et al (2015) SN2014J gamma rays from the ⁵⁶Ni decay chain. *Astronomy & Astrophysics* 574:A72. <https://doi.org/10.1051/0004-6361/201424991>, URL http://adsabs.harvard.edu/cgi-bin/nph-data_query?bibcode=2015A%26A...574A.72D&link_type=EJOURNAL
- Diehl R, Siebert T, Greiner J, et al (2018) INTEGRAL/SPI γ -ray line spectroscopy. Response and background characteristics. *Astronomy & Astrophysics* 611:A12. <https://doi.org/10.1051/0004-6361/201731815>, URL http://adsabs.harvard.edu/cgi-bin/nph-data_query?bibcode=2018A%26A...611A.12D&link_type=EJOURNAL

- Faherty J, Walter FM, Anderson J (2007) The trigonometric parallax of the neutron star Geminga 308:225–230. <https://doi.org/10.1007/s10509-007-9368-0>
- Ferrière K, Gillard W, Jean P (2007) Spatial distribution of interstellar gas in the innermost 3 kpc of our galaxy. *Astronomy and Astrophysics* 467(2):611–627. <https://doi.org/10.1051/0004-6361:20066992>
- Ferrière KM (2001) The interstellar environment of our galaxy. *Reviews of Modern Physics* 73:1031–1066. <https://doi.org/10.1103/RevModPhys.73.1031>
- Finkbeiner DP (2003) A full-sky h-alpha template for microwave foreground prediction. *The Astrophysical Journal Supplement Series* 146(2):407–415. <https://doi.org/10.1086/374411>
- Finkbeiner DP, Weiner N (2007) Exciting dark matter and the INTEGRAL/SPI 511keV signal. *Physical Review D* 76(8):083,519. <https://doi.org/10.1103/PhysRevD.76.083519>, URL http://adsabs.harvard.edu/cgi-bin/nph-data_query?bibcode=2007PhRvD..76h3519F&link_type=EJOURNAL
- Fox OD, Smith N, Ammons SM, et al (2015) What powers the 3000-day light curve of sn 2006gy? <https://doi.org/10.48550/ARXIV.1509.06407>
- Freudenreich HT (1998) A COBE Model of the Galactic Bar and Disk. *The Astrophysical Journal* 492(2):495–510. <https://doi.org/10.1086/305065>, URL <https://iopscience.iop.org/article/10.1086/305065>
- Gaensler BM, Madsen GJ, Chatterjee S, et al (2008) The vertical structure of warm ionised gas in the milky way. *Publications of the Astronomical Society of Australia* 25(4):184–200. <https://doi.org/10.1071/as08004>
- Genzel R, Schödel R, Ott T, et al (2003) The Stellar Cusp around the Supermassive Black Hole in the Galactic Center 594:812–832
- Geringer-Sameth A, Walker MG, Koushiappas SM, et al (2015) Indication of Gamma-Ray Emission from the Newly Discovered Dwarf Galaxy Reticulum II. *Physical Review Letters* 115(8):081,101. <https://doi.org/10.1103/PhysRevLett.115.081101>, URL <http://arxiv.org/abs/1503.02320>
- Ghez AM, Wright SA, Matthews K, et al (2004) Variable infrared emission from the supermassive black hole at the center of the milky way. *The Astrophysical Journal* 601(2):L159–L162. <https://doi.org/10.1086/382024>
- Goldwurm A, Ballet J, Cordier B, et al (1992) Sigma/GRANAT soft gamma-ray observations of the X-ray nova in Musca - Discovery of positron annihilation emission line 389:L79–L82. <https://doi.org/10.1086/186353>, URL <http://dx.doi.org/10.1086/186353>
- Gomez-Gomar J, Hernanz M, José J, et al (1998) Gamma-ray emission from individual classical novae 296:913–920. <https://doi.org/10.1046/j.1365-8711.1998.01421.x>
- Guessoum N, Jean P, Gillard W (2005) The lives and deaths of positrons in the interstellar medium. *Astronomy & Astrophysics* 436(1):171–185. <https://doi.org/10.1051/0004-6361:20042454>, URL http://adsabs.harvard.edu/cgi-bin/nph-data_query?bibcode=2005A%26A...436..171G&link_type=EJOURNAL
- Guessoum N, Jean P, Prantzos N (2006) Microquasars as sources of positron annihilation radiation. *Astronomy & Astrophysics* 457(3):753–762. <https://doi.org/10.1051/0004-6361:20065240>, URL <http://dx.doi.org/10.1051/0004-6361:20065240>
- Guessoum N, Jean P, Gillard W (2010) Positron annihilation on polycyclic aromatic hydrocarbon molecules in the interstellar medium. *arXiv.org* 402:1171–1178. <https://doi.org/10.1111/j.1365-2966.2009.15954.x>, URL <http://arxiv.org/abs/0911.0582>
- Harris WE (2010) A New Catalog of Globular Clusters in the Milky Way. *ArXiv e-prints astro-ph.GA*. URL <http://arxiv.org/abs/1012.3224>

- Harvey M, Rulden CB, Chadwick PM (2021) V404 cygni with fermi-LAT. *Monthly Notices of the Royal Astronomical Society* 506(4):6029–6038. <https://doi.org/10.1093/mnras/stab2097>
- Haslam CGT, Klein U, Salter CJ, et al (1981) A 408 MHz all-sky continuum survey. I - Observations at southern declinations and for the North Polar region 100:209–219
- Hawking S (1971) Gravitationally collapsed objects of very low mass. *Monthly Notices of the Royal Astronomical Society* 152:75–. <https://doi.org/10.1093/mnras/152.1.75>, URL http://adsabs.harvard.edu/cgi-bin/nph-data_query?bibcode=1971MNRAS.152...75H&link_type=EJOURNAL
- Hawking SW (1975) Particle creation by black holes. *Communications In Mathematical Physics* 43(3):199–220. <https://doi.org/10.1007/BF02345020>, URL http://adsabs.harvard.edu/cgi-bin/nph-data_query?bibcode=1975CMaPh..43..199H&link_type=EJOURNAL
- Haymes RC, Ellis DV, Fishman GJ, et al (1969) Observation of Hard Radiation from the Region of the Galactic Center 157:1455. <https://doi.org/10.1086/150164>
- Hernanz M (2014) Gamma-ray Emission from Nova Outbursts. In: Woudt PA, Ribeiro VARM (eds) arXiv.org, p 319, URL <http://arxiv.org/abs/1305.0769>
- Hernanz M, José J (2006) Radioactivities from novae 50:504–508. <https://doi.org/10.1016/j.newar.2006.06.012>
- Hernanz M, Smith DM, Fishman J, et al (2000) BATSE observations of classical novae. In: THE FIFTH COMPTON SYMPOSIUM. AIP Conference Proceedings, Institute for Spatial Studies of Catalonia (IEEC/C-SIC/UPC), Gran Capità 2-4, 08034 Barcelona (Spain). American Institute of Physics AIP, pp 82–86, <https://doi.org/10.1063/1.1303179>, URL http://adsabs.harvard.edu/cgi-bin/nph-data_query?bibcode=2000AIPC..510...82H&link_type=EJOURNAL
- Higdon JC, Lingenfelter RE, Rothschild RE (2009) The Galactic Positron Annihilation Radiation and the Propagation of Positrons in the Interstellar Medium. *The Astrophysical Journal* 698(1):350–379. <https://doi.org/10.1088/0004-637X/698/1/350>, URL http://adsabs.harvard.edu/cgi-bin/nph-data_query?bibcode=2009ApJ...698..350H&link_type=EJOURNAL
- Hooper D, Ferrer F, Boehm C, et al (2004) Possible Evidence for MeV Dark Matter in Dwarf Spheroidals. *Physical Review Letters* 93(16):161,302
- Iguaz J, Serpico PD, Siegert T (2021) Isotropic X-ray bound on Primordial Black Hole Dark Matter. arXiv.org p arXiv:2104.03145. URL <http://adsabs.harvard.edu/abs/2021arXiv210403145I>, <https://arxiv.org/abs/2104.03145>
- Iyudin AF, Diehl R, Lichti GG, et al (1997) Cas A in the Light of the 44Ti 1.15 MeV Gamma-Ray Line Emission. *The Transparent Universe* 382:37–37. URL <http://adsabs.harvard.edu/abs/1997ESASP.382...37I>
- Jean P, Knoedlseder J, Gillard W, et al (2006) Spectral analysis of the Galactic e+e- annihilation emission. *Astronomy & Astrophysics* 445(2):579–589. <https://doi.org/10.1051/0004-6361/20053765>, URL <https://www.aanda.org/articles/aa/abs/2006/02/aa3765-05/aa3765-05.html>
- Jean P, Gillard W, Marcowith A, et al (2009) Positron transport in the interstellar medium. *Astronomy & Astrophysics* 508(3):1099–1116. <https://doi.org/10.1051/0004-6361/200809830>, URL http://adsabs.harvard.edu/cgi-bin/nph-data_query?bibcode=2009A%26A...508.1099J&link_type=EJOURNAL
- Jerkstrand A, Maeda K, Kawabata K (2020) A type ia supernova at the heart of superluminous transient sn 2006gy <https://doi.org/10.48550/ARXIV.2002.10768>
- José J, Hernanz M (1998) Nucleosynthesis in Classical Novae: CO versus ONE White Dwarfs. *The Astrophysical Journal* 494(2):680–690.

- <https://doi.org/10.1086/305244>, URL <https://iopscience.iop.org/article/10.1086/305244>
- José J, Hernanz M, Coc A (2001) Classical novae: sources of CNO-nuclei and gamma-ray emitters. *Nuclear Physics A* 688:118–121. [https://doi.org/10.1016/S0375-9474\(01\)00680-7](https://doi.org/10.1016/S0375-9474(01)00680-7)
- Jourdain E, Roques JP, Rodi J (2017) A Challenging View of the 2015 Summer V404 Cyg Outburst at High Energy with INTEGRAL/SPI: The Finale. *arXivorg* 834:130. <https://doi.org/10.3847/1538-4357/834/2/130>, URL <http://arxiv.org/abs/1611.02890>
- Jungman G, Kamionkowski M, Griest K (1996) Supersymmetric dark matter 267:195–373. [https://doi.org/10.1016/0370-1573\(95\)00058-5](https://doi.org/10.1016/0370-1573(95)00058-5)
- Kerp J, Winkel B, Ben Bekhti N, et al (2011) The Effelsberg Bonn H I Survey (EBHIS). *Astronomische Nachrichten* 332:637. <https://doi.org/10.1002/asna.201011548>, URL <http://arxiv.org/abs/1104.1185>
- Knödseder J (1999) Implications of 1.8 MeV Gamma-Ray Observations for the Origin of 26Al. *The Astrophysical Journal* 510(2):915–929. <https://doi.org/10.1086/306601>, URL http://adsabs.harvard.edu/cgi-bin/nph-data_query?bibcode=1999ApJ...510..915K&link_type=EJOURNAL
- Knoedseder J, Jean P, Lonjou V, et al (2005) The all-sky distribution of 511 keV electron-positron annihilation emission. *Astronomy & Astrophysics* 441(2):513–532. <https://doi.org/10.1051/0004-6361:20042063>, URL <https://www.aanda.org/articles/aa/abs/2005/38/aa2063-04/aa2063-04.html>
- Kopp J (2013) Constraints on dark matter annihilation from AMS-02 results. *Physical Review D* 88(7):076,013. <https://doi.org/10.1103/physrevd.88.076013>
- Krause M, Fierlinger K, Diehl R, et al (2013) Feedback by massive stars and the emergence of superbubbles. I. Energy efficiency and Vishniac instabilities. *arXivorg* 550:A49. <https://doi.org/10.1051/0004-6361/201220060>, URL <https://www.aanda.org/articles/aa/abs/2013/02/aa20060-12/aa20060-12.html>
- Krause MGH, Diehl R, Bagetakos Y, et al (2015) 26Al kinematics: superbubbles following the spiral arms?. Constraints from the statistics of star clusters and HI superbubbles. *Astronomy & Astrophysics* 578:A113. <https://doi.org/10.1051/0004-6361/201525847>, URL http://adsabs.harvard.edu/cgi-bin/nph-data_query?bibcode=2015A%26A...578A.113K&link_type=EJOURNAL
- Krause MGH, Rodgers-Lee D, Dale JE, et al (2021) Galactic 26Al traces metal loss through hot chimneys. *Monthly Notices of the Royal Astronomical Society* 501(1):210–218. <https://doi.org/10.1093/mnras/staa3612>, URL http://adsabs.harvard.edu/cgi-bin/nph-data_query?bibcode=2021MNRAS.501..210K&link_type=EJOURNAL
- Laha R, Muñoz JB, Slatyer TR (2020) INTEGRAL constraints on primordial black holes and particle dark matter. *Physical Review D* 101(1):123,514. <https://doi.org/10.1103/PhysRevD.101.123514>, URL http://adsabs.harvard.edu/cgi-bin/nph-data_query?bibcode=2020PhRvD.10113514L&link_type=EJOURNAL
- Launhardt R, Zylka R, Mezger PG (2002) The nuclear bulge of the Galaxy. III. Large-scale physical characteristics of stars and interstellar matter. *Astronomy & Astrophysics* 384(1):112–139. <https://doi.org/10.1051/0004-6361:20020017>, URL http://adsabs.harvard.edu/cgi-bin/nph-data_query?bibcode=2002A%26A...384..112L&link_type=EJOURNAL
- Leung SC, Siegert T (2022) Gamma-ray light curves and spectra of classical novae. *MNRAS* 516(1):1008–1021. <https://doi.org/10.1093/mnras/stac1672>, URL <https://ui.adsabs.harvard.edu/abs/2022MNRAS.516.1008L>, <https://arxiv.org/abs/2112.06893> [astro-ph.HE]
- Leventhal M, MacCallum CJ, Stang PD (1978) Detection of 511 keV positron annihilation radiation from the galactic center direction. *Astrophysical Journal* 225:L11–L14. <https://doi.org/10.1086/182782>, URL <http://adsabs.harvard.edu/abs/1978ApJ...225L..11L>

- edu/abs/1978ApJ...225L..11L
- Lightman AP, Zdziarski AA (1987) Pair production and Compton scattering in compact sources and comparison to observations of active galactic nuclei 319:643–661. <https://doi.org/10.1086/165485>
- Lin RP, Dennis BR, Hurford GJ, et al (2002) The reuven ramaty high-energy solar spectroscopic imager (rhessi) 210(1):3–32. <https://doi.org/10.1023/A:1022428818870>, URL <https://ui.adsabs.harvard.edu/abs/2002SoPh..210....3L>
- Lingenfelter RE, Ramaty R (1989) The nature of the annihilation radiation and gamma-ray continuum from the Galactic center region. *Astrophysical Journal* 343:686–695. <https://doi.org/10.1086/167740>, URL <http://adsabs.harvard.edu/doi/10.1086/167740>
- Maciolek-Niedzwiecki A, Zdziarski AA, Coppi PS (1995) Electron / Positron Pair Production and Annihilation Spectral Features from Compact Sources 276:273. <https://doi.org/10.1093/mnras/276.1.273>
- Martin P, Vink J (2008) Linking 44Ti explosive nucleosynthesis to the dynamics of core-collapse supernovae 52:401–404
- Martin P, Strong AW, Jean P, et al (2012) Galactic annihilation emission from nucleosynthesis positrons. *Astronomy & Astrophysics* 543:A3. <https://doi.org/10.1051/0004-6361/201118721>, URL http://adsabs.harvard.edu/cgi-bin/nph-data_query?bibcode=2012A%26A...543A..3M&link_type=EJOURNAL
- Maximon LC, Olsen H (1962) Measurement of Linear Photon Polarization by Pair Production. *Phys Rev* 126(1):310. <https://doi.org/10.1103/PhysRev.126.310>, URL <https://journals.aps.org/pr/abstract/10.1103/PhysRev.126.310>
- Milne PA, The LS, Leising MD (1999) Positron Escape from Type IA Supernovae 124:503–526. <https://doi.org/10.1086/313262>
- Morris M, Serabyn E (1996) The Galactic Center Environment 34:645–702. <https://doi.org/10.1146/annurev.astro.34.1.645>
- Moskalenko IV, Porter TA (2007) The Gamma-Ray Albedo of the Moon. *The Astrophysical Journal* 670(2):1467–1472. <https://doi.org/10.1086/522828>, URL http://adsabs.harvard.edu/cgi-bin/nph-data_query?bibcode=2007ApJ...670.1467M&link_type=EJOURNAL
- Moskalenko IV, Strong AW (1998) Production and Propagation of Cosmic-Ray Positrons and Electrons 493:694–707. <https://doi.org/10.1086/305152>
- Moskalenko IV, Porter TA, Digel SW, et al (2008) A Celestial Gamma-Ray Foreground Due to the Albedo of Small Solar System Bodies and a Remote Probe of the Interstellar Cosmic-Ray Spectrum. *The Astrophysical Journal* 681(2):1708–1716. <https://doi.org/10.1086/588425>, URL http://adsabs.harvard.edu/cgi-bin/nph-data_query?bibcode=2008ApJ...681.1708M&link_type=EJOURNAL
- Murphy RJ, Dermer CD, Ramaty R (1987) High-energy processes in solar flares. *The Astrophysical Journal Supplement Series* 63:721. <https://doi.org/10.1086/191180>
- Murphy RJ, Share GH, Skibo JG, et al (2005) The Physics of Positron Annihilation in the Solar Atmosphere. *The Astrophysical Journal Supplement Series* 161(2):495–519. <https://doi.org/10.1086/452634>, URL <https://iopscience.iop.org/article/10.1086/452634>
- Murphy RJ, Kozlovsky B, Share GH (2014) Radioactive Positron Emitter Production by Energetic Alpha Particles in Solar Flares. *The Astrophysical Journal Supplement* 215(2):18. <https://doi.org/10.1088/0067-0049/215/2/18>, URL http://adsabs.harvard.edu/cgi-bin/nph-data_query?bibcode=2014ApJS..215...18M&link_type=EJOURNAL
- and N. Aghanim, Ashdown M, Aumont J, et al (2016) Planck intermediate resultsxlvi. disentangling galactic dust emission and cosmic infrared background anisotropies. *Astronomy and Astrophysics* 596:A109. <https://doi.org/10.1051/0004-6361/201629022>

- Ng KCY, Roach BM, Perez K, et al (2019) New constraints on sterile neutrino dark matter from NuSTAR M31 observations. *Physical Review D* 99(8):083,005. <https://doi.org/10.1103/PhysRevD.99.083005>, URL http://adsabs.harvard.edu/cgi-bin/nph-data_query?bibcode=2019PhRvD..99h3005N&link_type=EJOURNAL
- Ore A, Powell JL (1949) Three-Photon Annihilation of an Electron-Positron Pair. *Physical Review* 75:1696–1699. <https://doi.org/10.1103/PhysRev.75.1696>
- Panther F (2018) Positron Transport and Annihilation in the Galactic Bulge. *Galaxies* 6:39. <https://doi.org/10.3390/galaxies6020039>, URL <http://arxiv.org/abs/1801.09365>
- Panther FH, Crocker RM, Birnboim Y, et al (2018a) Positron annihilation in the nuclear outflows of the Milky Way. *Monthly Notices of the Royal Astronomical Society: Letters* 474(1):L17–L21. <https://doi.org/10.1093/mnrasl/slx183>, URL http://adsabs.harvard.edu/cgi-bin/nph-data_query?bibcode=2018MNRAS.474L..17P&link_type=EJOURNAL
- Panther FH, Seitzzahl IR, Crocker RM, et al (2018b) Effect of positron-alkali metal atom interactions in the diffuse interstellar medium. *Physical Review D* 98(2):023,015. <https://doi.org/10.1103/PhysRevD.98.023015>, URL http://adsabs.harvard.edu/cgi-bin/nph-data_query?bibcode=2018PhRvD..98b3015P&link_type=EJOURNAL
- Panther FH, Seitzzahl IR, Ruiter AJ, et al (2021) Prospects of direct detection of 48v gamma-rays from thermonuclear supernovae. *Monthly Notices of the Royal Astronomical Society* 508(2):1590–1598. <https://doi.org/10.1093/mnras/stab2701>
- Peplowski PN (2016) The global elemental composition of 433 eros: First results from the NEAR gamma-ray spectrometer orbital dataset. *Planetary and Space Science* 134:36–51. <https://doi.org/10.1016/j.pss.2016.10.006>
- Planck Collaboration, Adam R, Ade PAR, et al (2016) Planck 2015 results. X. Diffuse component separation: Foreground maps. *arXivorg* 594:A10. <https://doi.org/10.1051/0004-6361/201525967>, URL <http://arxiv.org/abs/1502.01588>
- Pleintinger MMM (2020) Star Groups and their Nucleosynthesis. PhD Dissertation URL http://adsabs.harvard.edu/cgi-bin/nph-data_query?bibcode=2020PhDT.....13P&link_type=EJOURNAL
- Pleintinger MMM, Siebert T, Diehl R, et al (2019) Comparing simulated 26Al maps to gamma-ray measurements. *Astronomy & Astrophysics* 632:A73. <https://doi.org/10.1051/0004-6361/201935911>, URL http://adsabs.harvard.edu/cgi-bin/nph-data_query?bibcode=2019A%26A...632A..73P&link_type=EJOURNAL
- Portegies Zwart SF, Verbunt F, Ergma E (1997) The formation of black-holes in low-mass X-ray binaries. 321:207–212
- Porter TA, Moskalenko IV, Strong AW, et al (2008) Inverse Compton Origin of the Hard X-Ray and Soft Gamma-Ray Emission from the Galactic Ridge. *arXivorg* 682(1):400–407. <https://doi.org/10.1086/589615>, URL <http://arxiv.org/abs/0804.1774>
- Prantzos N (2004) Astrophysical Gamma-Ray Lines: A Probe of Stellar Nucleosynthesis and Star Formation. In: Schoenfelder V, Lichti G, Winkler C (eds) 5th INTEGRAL Workshop on the INTEGRAL Universe, p 15
- Prantzos N (2006) On the intensity and spatial morphology of the 511 keV emission in the Milky Way. *Astronomy & Astrophysics* 449(3):869–878. <https://doi.org/10.1051/0004-6361:20052811>, URL <https://www.aanda.org/articles/aa/abs/2006/15/aa2811-05/aa2811-05.html>
- Prantzos N, Boehm C, Bykov AM, et al (2011) The 511 keV emission from positron annihilation in the Galaxy. *Reviews of Modern Physics* 83(3):1001–1056. <https://doi.org/10.1103/RevModPhys.83.1001>

- URL <https://journals.aps.org/rmp/abstract/10.1103/RevModPhys.83.1001>
- Purcell WR, Cheng LX, Dixon DD, et al (1997) OSSE Mapping of Galactic 511 keV Positron Annihilation Line Emission. *The Astrophysical Journal* 491(2):725–748. <https://doi.org/10.1086/304994>, URL http://adsabs.harvard.edu/cgi-bin/nph-data_query?bibcode=1997ApJ...491..725P&link_type=EJOURNAL
- Quataert E (2004) A Dynamical Model for Hot Gas in the Galactic Center 613:322–325. <https://doi.org/10.1086/422973>
- Renaud M, Vink J, Decourchelle A, et al (2006) The Signature of ⁴⁴Ti in Cassiopeia A Revealed by IBIS/ISGRI on INTEGRAL 647:L41–L44
- Rodriguez J, Cadolle Bel M, Alfonso-Garzón J, et al (2015) Correlated optical, X-ray, and γ -ray flaring activity seen with INTEGRAL during the 2015 outburst of V404 Cygni. *arXivorg* 581:L9. <https://doi.org/10.1051/0004-6361/201527043>, URL <http://arxiv.org/abs/1507.06659>
- Romani RW (1992) Populations of low-mass black hole binaries 399:621–626. <https://doi.org/10.1086/171953>
- Roques JP, Jourdain E, Bazzano A, et al (2015) First INTEGRAL Observations of V404 Cygni during the 2015 Outburst: Spectral Behavior in the 20-650 keV Energy Range. *arXivorg* 813:L22. <https://doi.org/10.1088/2041-8205/813/1/L22>, URL <http://arxiv.org/abs/1510.03677>
- Rothschild RE (2009) Positron propagation and the INTEGRAL/SPI 511 keV bulge/disk ratio. In: *Proceedings of 7th INTEGRAL Workshop — PoS(Integral08)*. Sissa Medialab, <https://doi.org/10.22323/1.067.0028>
- Saxena S, Summa A, Elsässer D, et al (2011) Constraints on dark matter annihilation from m87: Signatures of prompt and inverse-compton gamma rays <https://doi.org/10.1140/epjc/s10052-011-1815-y>, <https://arxiv.org/abs/1111.3868> [astro-ph.HE]
- Seaton MJ (1959) Radiative recombination of hydrogenic ions 119:81. <https://doi.org/10.1093/mnras/119.2.81>
- Seitzzahl IR, Timmes FX, Magkotsios G (2014) The Light Curve of SN 1987A Revisited: Constraining Production Masses of Radioactive Nuclides. *arXivorg* 792:10. URL <http://arxiv.org/abs/1408.5986>
- Serpico PD (2011) Astrophysical models for the origin of the positron "excess" <https://doi.org/10.1016/j.astropartphys.2011.08.007>, <https://arxiv.org/abs/1108.4827> [astro-ph.HE]
- Shafter AW (2017) The Galactic Nova Rate Revisited. *arXivorg* 834(2):196. <https://doi.org/10.3847/1538-4357/834/2/196>, URL <http://arxiv.org/abs/1606.02358>
- Share GH, Murphy RJ, Smith DM, et al (2004) RHESSI e⁺-e⁻ Annihilation Radiation Observations: Implications for Conditions in the Flaring Solar Chromosphere 615:L169–L172. <https://doi.org/10.1086/426478>
- Shibayama T, Maehara H, Notsu S, et al (2013) Superflares on Solar-type Stars Observed with Kepler. I. Statistical Properties of Superflares. *The Astrophysical Journal Supplement* 209(1):5. <https://doi.org/10.1088/0067-0049/209/1/5>, URL http://adsabs.harvard.edu/cgi-bin/nph-data_query?bibcode=2013ApJS..209...5S&link_type=EJOURNAL
- Siegert T (2017) Positron-Annihilation Spectroscopy throughout the Milky Way. PhD thesis, Technische Universität München, Published online at <https://mediatum.ub.tum.de/node?id=1340342>
- Siegert T, Diehl R, Krause MGH, et al (2015) Revisiting INTEGRAL/SPI observations of ⁴⁴Ti from Cassiopeia A. *Astronomy & Astrophysics* 579:A124. <https://doi.org/10.1051/0004-6361/201525877>, URL http://adsabs.harvard.edu/cgi-bin/nph-data_query?bibcode=2015A%26A...579A.124S&link_type=EJOURNAL

- Siegert T, Diehl R, Greiner J, et al (2016a) Positron annihilation signatures associated with the outburst of the microquasar V404 Cygni. *Nature* 531(7):341–343. <https://doi.org/10.1038/nature16978>, URL http://adsabs.harvard.edu/cgi-bin/nph-data_query?bibcode=2016Natur.531..341S&link_type=EJOURNAL
- Siegert T, Diehl R, Khachatryan G, et al (2016b) Gamma-ray spectroscopy of positron annihilation in the Milky Way. *Astronomy & Astrophysics* 586:A84. <https://doi.org/10.1051/0004-6361/201527510>, URL http://adsabs.harvard.edu/cgi-bin/nph-data_query?bibcode=2016A%26A...586A..84S&link_type=EJOURNAL
- Siegert T, Diehl R, Vincent AC, et al (2016c) Search for 511 keV emission in satellite galaxies of the Milky Way with INTEGRAL/SPI. *Astronomy & Astrophysics* 595:A25. <https://doi.org/10.1051/0004-6361/201629136>, URL http://adsabs.harvard.edu/cgi-bin/nph-data_query?bibcode=2016A%26A...595A..25S&link_type=EJOURNAL
- Siegert T, Crocker RM, Diehl R, et al (2019a) Constraints on positron annihilation kinematics in the inner Galaxy. *Astronomy & Astrophysics* 627:A126. <https://doi.org/10.1051/0004-6361/201833856>, URL http://adsabs.harvard.edu/cgi-bin/nph-data_query?bibcode=2019A%26A...627A.126S&link_type=EJOURNAL
- Siegert T, Diehl R, Weinberger C, et al (2019b) Background modelling for γ -ray spectroscopy with INTEGRAL/SPI. *Astronomy & Astrophysics* 626:A73. <https://doi.org/10.1051/0004-6361/201834920>, URL http://adsabs.harvard.edu/cgi-bin/nph-data_query?bibcode=2019A%26A...626A..73S&link_type=EJOURNAL
- Siegert T, Boehm C, Calore F, et al (2021a) Reticulum II: Particle Dark Matter and Primordial Black Holes Limits. arXiv preprint arXiv:2109.03791. URL <http://adsabs.harvard.edu/abs/2021arXiv210903791S>, <https://arxiv.org/abs/2109.03791>
- Siegert T, Crocker RM, Macias O, et al (2021b) Measuring the smearing of the Galactic 511 keV signal: positron propagation or supernova kicks? arXiv preprint arXiv:2109.03691. <https://doi.org/10.1093/mnrasl/slab113>, URL <http://adsabs.harvard.edu/abs/2021arXiv210903691S>, <https://arxiv.org/abs/2109.03691> [astro-ph.HE]
- Siegert T, Ghosh S, Mathur K, et al (2021c) Nucleosynthesis constraints through γ -ray line measurements from classical novae. arXiv preprint arXiv:2104.00363. URL <http://adsabs.harvard.edu/abs/2021arXiv210400363S>, <https://arxiv.org/abs/2104.00363>
- Siegert T, Berteaud J, Calore F, et al (2022a) Diffuse Galactic emission spectrum between 0.5 and 8.0 MeV. arXiv preprint arXiv:2202.04574. URL <http://adsabs.harvard.edu/abs/2022arXiv220204574S>, <https://arxiv.org/abs/2202.04574>
- Siegert T, Boehm C, Calore F, et al (2022b) An integral/spi view of reticulum ii: particle dark matter and primordial black holes limits in the mev range. *MNRAS* 511(1):914–924. <https://doi.org/10.1093/mnras/stac008>, URL <https://ui.adsabs.harvard.edu/abs/2022MNRAS.511..914S>, <https://arxiv.org/abs/2109.03791> [astro-ph.HE]
- Siegert T, Crocker RM, Macias O, et al (2022c) Measuring the smearing of the Galactic 511-keV signal: positron propagation or supernova kicks? *MNRAS* 509(1):L11–L16. <https://doi.org/10.1093/mnrasl/slab113>, URL http://adsabs.harvard.edu/cgi-bin/nph-data_query?bibcode=2022MNRAS.509L..11S&link_type=EJOURNAL
- Siegert T, Horan D, Kanbach G (2022d) Telescope concepts in gamma-ray astronomy arXiv:2207.02248. URL <https://ui.adsabs.harvard.edu/abs/2022arXiv220702248S>, <https://arxiv.org/abs/2207.02248>
- Sizun P, Cassé M, Schanne S (2006) Continuum γ -ray emission from light dark matter positrons and electrons. *Phys Rev D* 74(6):063,514. <https://doi.org/10.1103/PhysRevD.74.063514>, URL <https://journals.aps.org/prd/abstract/10.1103/PhysRevD.74.063514>

- Skinner G, Diehl R, Zhang X, et al (2014) The Galactic distribution of the 511 keV e⁺/e⁻ annihilation radiation. In: Proceedings of the 10th INTEGRAL Workshop: "A Synergistic View of the High-Energy Sky" (INTEGRAL 2014). 15-19 September 2014. Annapolis, MD, USA. Published online at <http://pos.sissa.it/cgi-bin/reader/conf.cgi?confid=228>, id.054, p 054
- Slatyer TR (2016) Indirect dark matter signatures in the cosmic dark ages. I. Generalizing the bound on s-wave dark matter annihilation from Planck results. *Physical Review D* 93(2):023,527. <https://doi.org/10.1103/PhysRevD.93.023527>, URL http://adsabs.harvard.edu/cgi-bin/nph-data_query?bibcode=2016PhRvD..93b3527S&link_type=EJOURNAL
- Smith N, Li W, Foley RJ, et al (2007) SN 2006gy: Discovery of the Most Luminous Supernova Ever Recorded, Powered by the Death of an Extremely Massive Star like η Carinae 666:1116–1128. <https://doi.org/10.1086/519949>
- Stritzinger M, Leibundgut B, Walch S, et al (2006) Constraints on the progenitor systems of type Ia supernovae 450:241–251
- Strong AW, Moskalenko IV, Ptuskin VS (2007) Cosmic-Ray Propagation and Interactions in the Galaxy. *Annual Review of Nuclear and Particle Science* 57(1):285–327. <https://doi.org/10.1146/annurev.nucl.57.090506.123011>, URL http://adsabs.harvard.edu/cgi-bin/nph-data_query?bibcode=2007ARNPS..57.285S&link_type=EJOURNAL
- Su M, Slatyer TR, Finkbeiner DP (2010) Giant Gamma-ray Bubbles from Fermi-LAT: Active Galactic Nucleus Activity or Bipolar Galactic Wind? *The Astrophysical Journal* 724(2):1044–1082. <https://doi.org/10.1088/0004-637X/724/2/1044>, URL http://adsabs.harvard.edu/cgi-bin/nph-data_query?bibcode=2010ApJ...724.1044S&link_type=EJOURNAL
- Sunyaev R, Churazov E, Gilfanov M, et al (1991) Three spectral states of 1E 1740.7 - 2942 - From standard Cygnus X-1 type spectrum to the evidence of electron-positron annihilation feature 383:L49–L52. <https://doi.org/10.1086/186238>, URL <http://adsabs.harvard.edu/doi/10.1086/186238>
- Svensson R (1982a) Electron-positron pair equilibria in relativistic plasmas. *ApJ* 258:335. <https://doi.org/10.1086/160082>, URL <https://ui.adsabs.harvard.edu/abs/1982ApJ...258..335S>
- Svensson R (1982b) The pair annihilation process in relativistic plasmas. *ApJ* 258:321–334. <https://doi.org/10.1086/160081>, URL <http://adsabs.harvard.edu/doi/10.1086/160081>
- Svensson R (1983) The thermal pair annihilation spectrum - A detailed balance approach 270:300–304. <https://doi.org/10.1086/161122>, URL <http://adsabs.harvard.edu/doi/10.1086/161122>
- Svensson R (1987) Non-thermal pair production in compact X-ray sources - First-order Compton cascades in soft radiation fields 227:403–451. <https://doi.org/10.1093/mnras/227.2.403>
- Tomsick JA, Zoglauer A, Sleator C, et al (2019) The Compton Spectrometer and Imager. arXiv:1908.04334. URL <http://adsabs.harvard.edu/abs/2019arXiv190804334T>
- Totani T, Oda T, Sumi T, et al (2006) Rapid Variability of Serendipitously Discovered Very Low-Luminosity AGNs and Implications for Accretion Disk Theory. In: Gaskell CM, McHardy IM, Peterson BM, et al (eds) *Astronomical Society of the Pacific Conference Series*, p 55
- Türler M, Chernyakova M, Courvoisier TJJ, et al (2010) INTEGRAL hard X-ray spectra of the cosmic X-ray background and Galactic ridge emission. *Astronomy & Astrophysics* 512:A49. <https://doi.org/10.1051/0004-6361/200913072>, URL http://adsabs.harvard.edu/cgi-bin/nph-data_query?bibcode=2010A%26A...512A..49T&link_type=EJOURNAL
- Vedrenne G, Roques JP, Schönfelder V, et al (2003) SPI: The spectrometer aboard INTEGRAL. *Astronomy & Astrophysics* 411(1):L63–L70. <https://doi.org/10.1051/0004-6361:20031482>,

URL http://adsabs.harvard.edu/cgi-bin/nph-data_query?bibcode=2003A%26A...411L.63V&link_type=EJOURNAL

Weaver R, McCray R, Castor J, et al (1977) Interstellar bubbles. II - Structure and evolution 218:377–395. <https://doi.org/10.1086/155692>

Weidenspointner G, Jean P, Knödelseder J, et al (200) New Clues to the Origin of Galactic Positrons. In: Barret D, Casoli F, Lagache G, et al (eds) SF2A-2006: Semaine de l’Astrophysique Francaise, pp 213—

Weidenspointner G, Skinner G, Jean P, et al (2008) An asymmetric distribution of positrons in the Galactic disk revealed by γ -rays. *Nature* 451(7):159–162. <https://doi.org/10.1038/nature06490>, URL http://adsabs.harvard.edu/cgi-bin/nph-data_query?bibcode=2008Natur.451.159W&link_type=EJOURNAL

Weinberger C, Diehl R, Pleintinger MMM, et al (2020) 44Ti ejecta in young supernova remnants. *Astronomy & Astrophysics* 638:A83. <https://doi.org/10.1051/0004-6361/202037536>, URL http://adsabs.harvard.edu/cgi-bin/nph-data_query?bibcode=2020A%26A...638A.83W&link_type=EJOURNAL

Winkler C, Courvoisier TJJ, Di Cocco G, et al (2003) The INTEGRAL mission. *Astronomy & Astrophysics* 411(1):L1–L6. <https://doi.org/10.1051/0004-6361:20031288>, URL <https://www.aanda.org/articles/aa/abs/2003/43/aaINTEGRAL9/aaINTEGRAL9.html>

Yin PF, Yu ZH, Yuan Q, et al (2013) Pulsar interpretation for the AMS-02 result. *arXivorg* 88(2):023,001. <https://doi.org/10.1103/PhysRevD.88.023001>, URL <http://arxiv.org/abs/1304.4128>

Zhang L, Cheng KS (1997) High-Energy Radiation from Rapidly Spinning Pulsars with Thick Outer Gaps 487:370–379